

Supplementary data

The tree species were abbreviated in the analyses: Qr – *Quercus robur*, Cb – *Carpinus betulus*, Tc – *Tilia cordata*, Fe – *Fraxinus excelsior*, Ac – *Acer campestre*, Pa – *Prunus avium*, and Ap – *Acer pseudoplatanus*.

Jaccard co-occurrence index

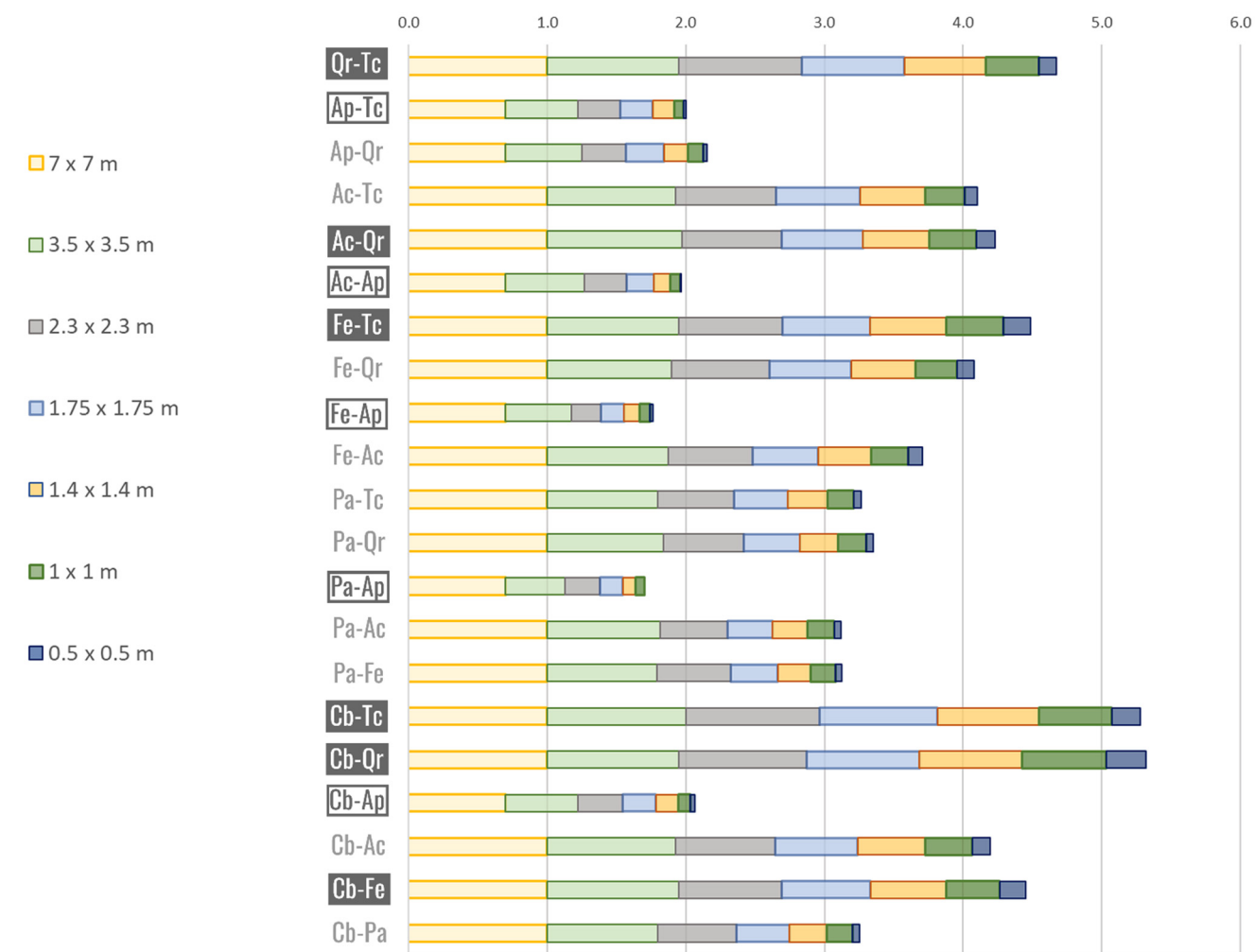


Figure S1. The variation of cumulative values of the Jaccard co-occurrence index describing pair-species associations for different quadrat sizes

Note. Species relationships with the most significant positive associations are marked with solid dark-grey labels, and those with the most significant negative associations are with white labels.

Table S1. The species compositions of the plots

Species percentage (%) in the plot							
Plot	Cb	Qr	Tc	Fe	Ac	Pa	Ap
1	37.5	45.0	8.5	3.0	3.5	2.0	0.5
2	57.5	29.0	4.0	1.0	3.5	1.0	4.0
3	70.0	4.0	15.0	4.5	4.5	1.0	1.0
4	74.5	2.5	11.5	2.0	5.5	3.0	1.0
5	61.0	22.0	5.0	3.0	8.0	1.0	0.0
6	74.0	1.5	14.0	8.0	1.5	1.0	0.0
7	34.0	4.5	21.0	35.0	3.5	1.5	0.5
8	61.0	24.0	6.0	1.5	4.5	1.0	2.0
9	51.0	15.0	9.5	3.0	18.5	3.0	0.0
10	53.0	10.0	10.0	17.5	6.0	3.5	0.0
Percentage of the species for the whole sampling	55	16	11	9	6	2	1

Table S2. The sapling's average height per species

	Cb	Qr	Tc	Fe	Ac	Pa	Ap
Average height (cm)	102.89	77.62	122.16	65.32	108.42	111.94	105.76
Coefficient of variation	48.8%	49.6%	38.7%	56.7%	41.7%	45.8%	55.7%

Table S3. Synthesis of information about the parent stand

	Qr	Cb	Tc	Fe
Species percentage	50%	30%	10%	10%
Age (years)	130	110	110	110
DBH (cm)	54	38	42	46
Canopy cover	0.6			

Principal component analysis

Table S4. The explained variance of PCA for different quadrat sizes and the most significant pair-species correlation

Qdrt. size	Nr. of qdts.	Proportion of variance		Pair-species correlation	
		PC1	PC2	Positive correlation	Negative correlation
7 × 7 m	10	35.7%	23.4%	Fe-Tc Pa-Ac Qr-Ap	Fe-Ap Tc-Ap Cb-Ac Cb-Qr
3.5 × 3.5 m	40	30%	19.1%	Fe-Tc Pa-Ac Qr-Ac	Fe-Ap Tc-Ap Cb-Ac Cb-Qr Pa-Ap
2.33 × 2.33 m	90	27.7%	19.4%	Fe-Tc Pa-Ac Qr-Ac Qr-Ap	Fe-Ap Tc-Ap Cb-Ac Cb-Qr
1.75 × 1.75 m	160	24%	18.5%	Fe-Tc Pa-Ac Qr-Ac	Fe-Ap Tc-Ap Cb-Ac Cb-Qr
1.4 × 1.4 m	250	21.7%	17.9%	Fe-Tc Pa-Ac	Fe-Ap Tc-Ap Cb-Ac Cb-Pa
1 × 1 m	489	20.2%	16.7%	Fe-Tc Pa-Ac Qr-Ac Qr-Ap	Fe-Ap Tc-Ap Cb-Ac Cb-Pa
0.5 × 0.5 m	1746	17.4%	16.3%	Fe-Tc Pa-Ac Qr-Ac	Fe-Ap Tc-Ap Cb-Qr Cb-Ac

Biplots of the principal component analysis on the species' local abundance

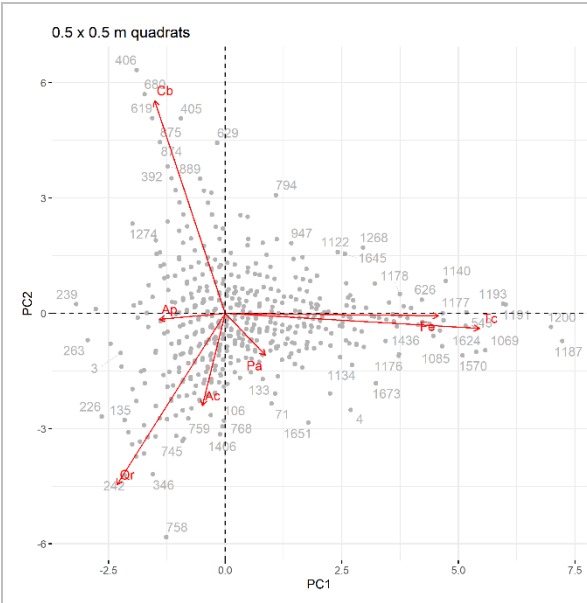


Figure S2. PCA biplot – 0.5 × 0.5 m quadrats

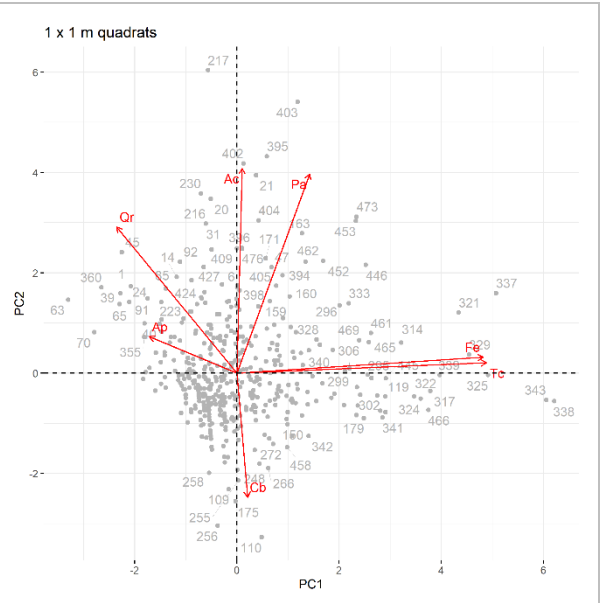


Figure S3. PCA biplot – 1 × 1 m quadrats

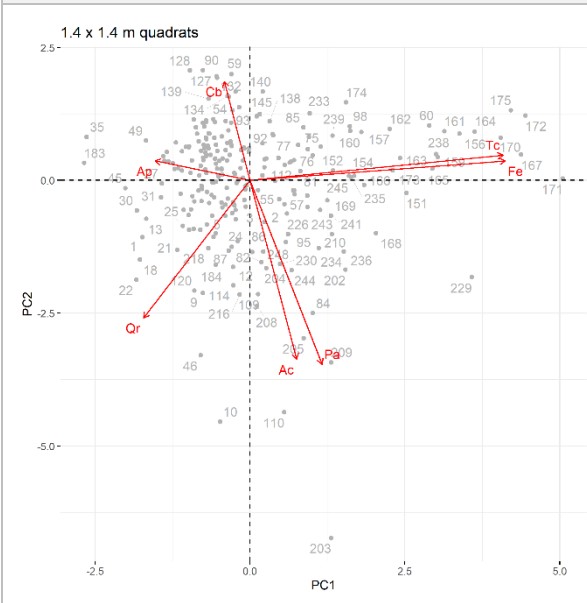


Figure S4. PCA biplot – 1.4 × 1.4 m quadrats

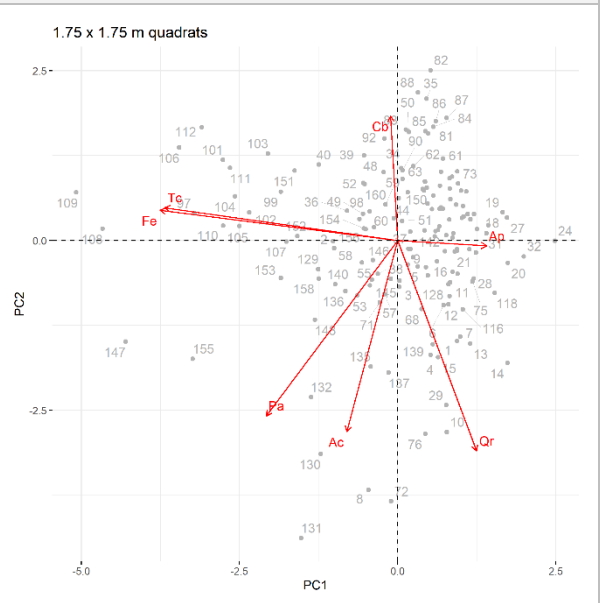


Figure S5. PCA biplot – 1.75 × 1.75 m quadrats

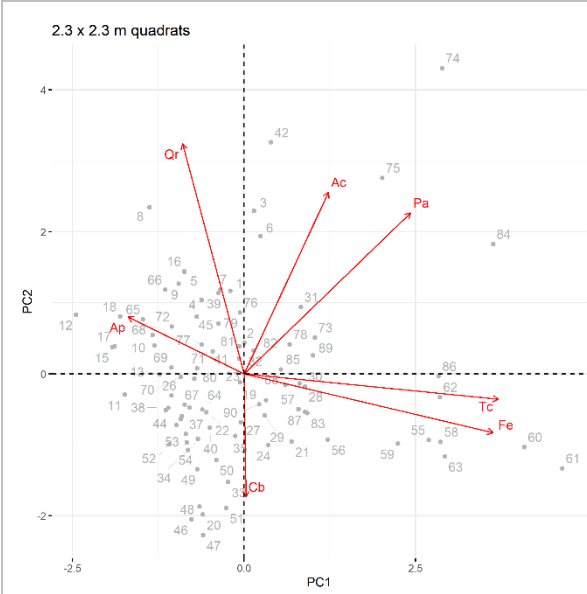


Figure S6. PCA biplot – 2.33 × 2.33 m quadrats

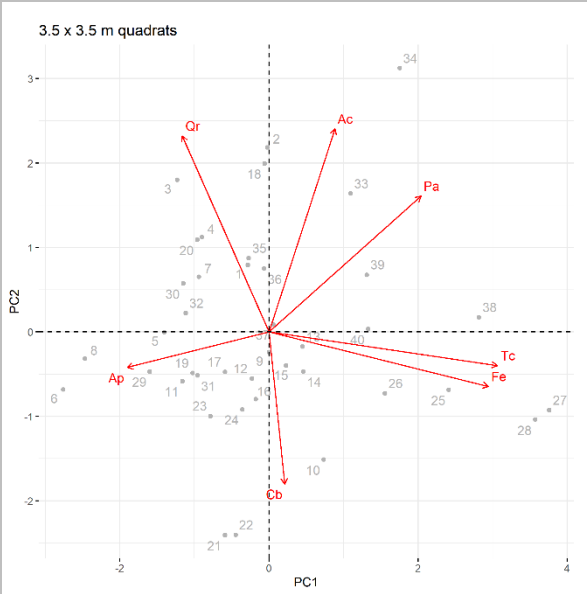


Figure S7. PCA biplot – 3.5 × 3.5 m quadrats

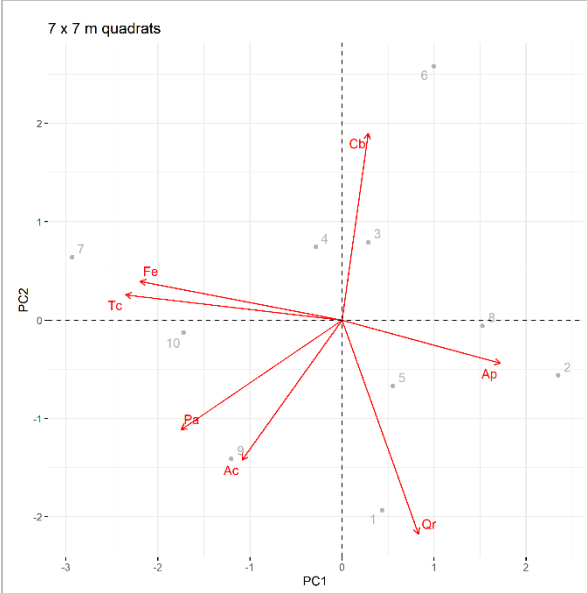


Figure S8. PCA biplot – 7 × 7 m quadrats

Synthesis of the bivariate analysis – Summary graphs for the significant species association ranges

Observation: The significant positive association ranges are marked with dark grey bars, while the negative ones are marked with light grey bars. Distances are given in centimetres. The circled plot numbers mark the plots with a significance level of probability lower than 0.05, considering the Cramer-von Mises test.

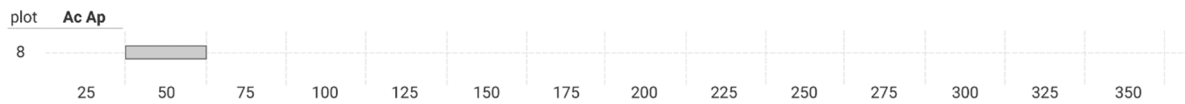


Figure S9. Ac–Ap significant association ranges

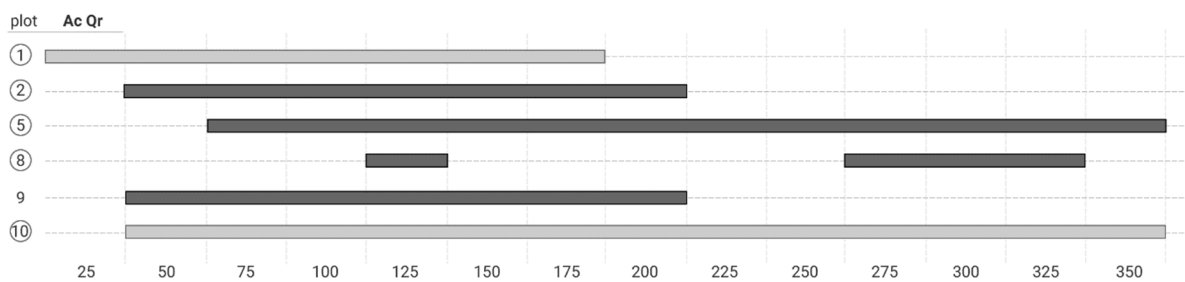


Figure S10. Ac–Qr significant association ranges

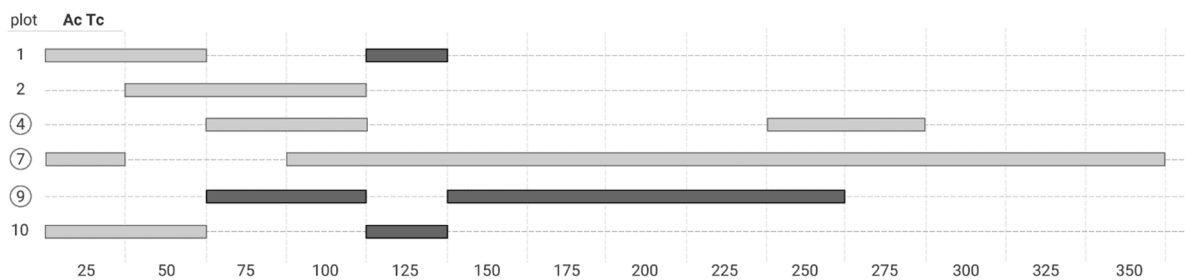


Figure S11. Ac–Tc significant association ranges

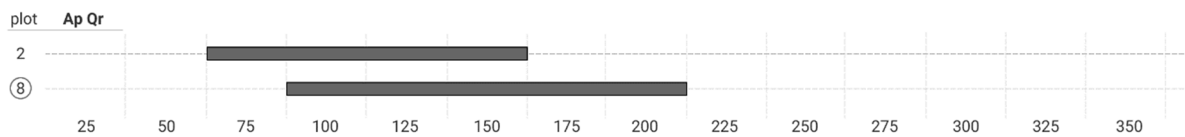


Figure S12. Ap–Qr significant association ranges

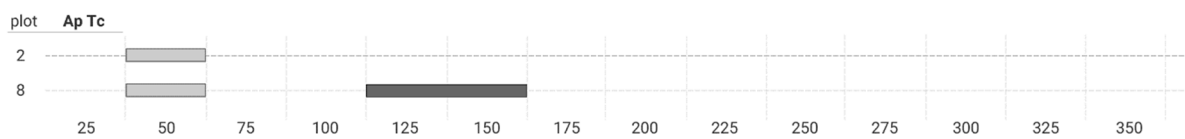


Figure S13. Ap–Tc significant association ranges

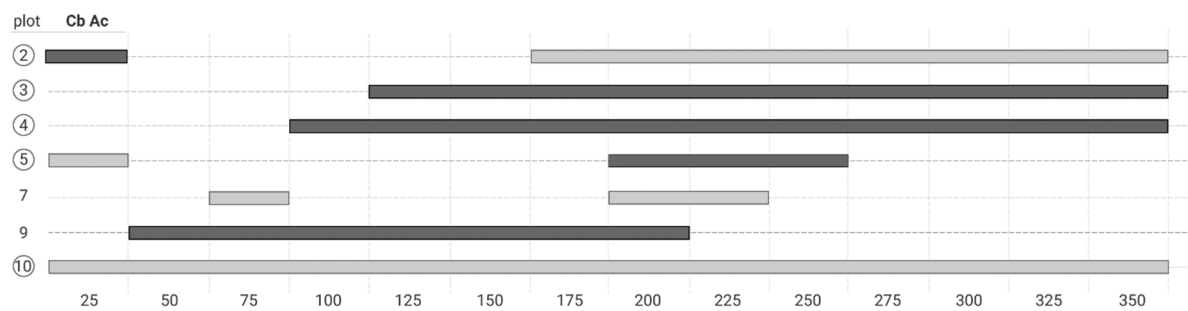


Figure S14. Cb–Ac significant association ranges

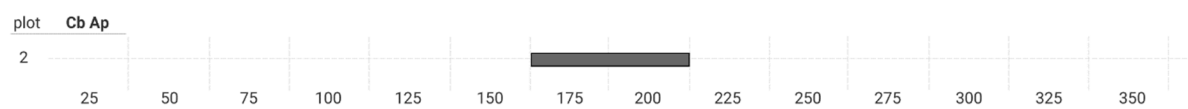


Figure S15. Cb–Ap significant association ranges

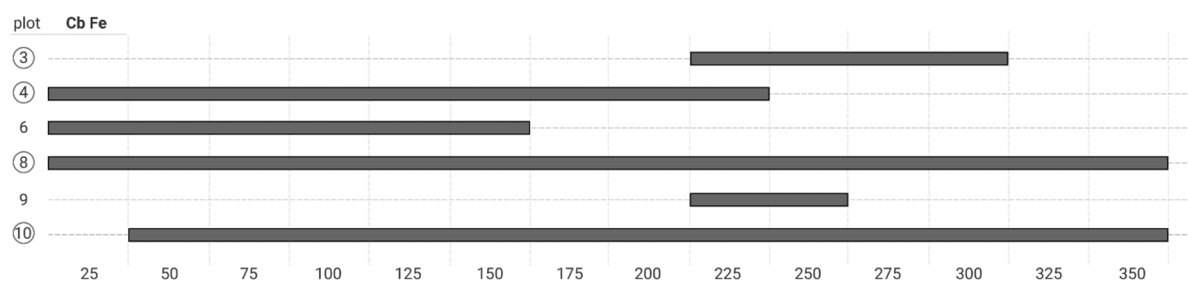


Figure S16. Cb–Fe significant association ranges

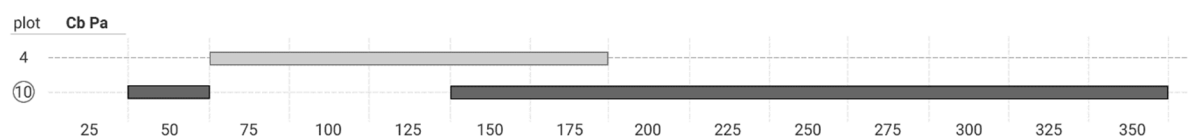


Figure S17. Cb–Pa significant association ranges

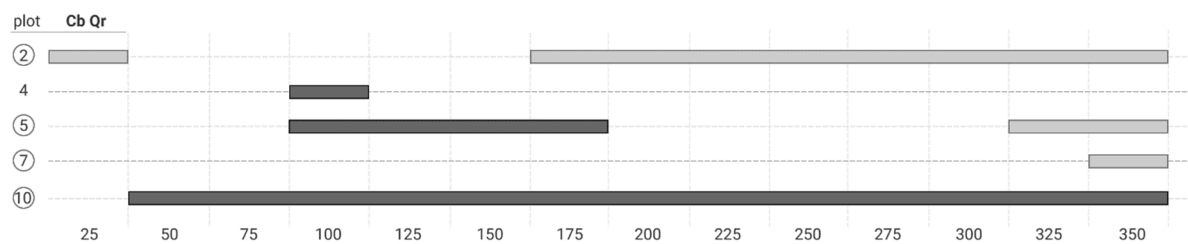


Figure S18 Cb–Qr significant association ranges

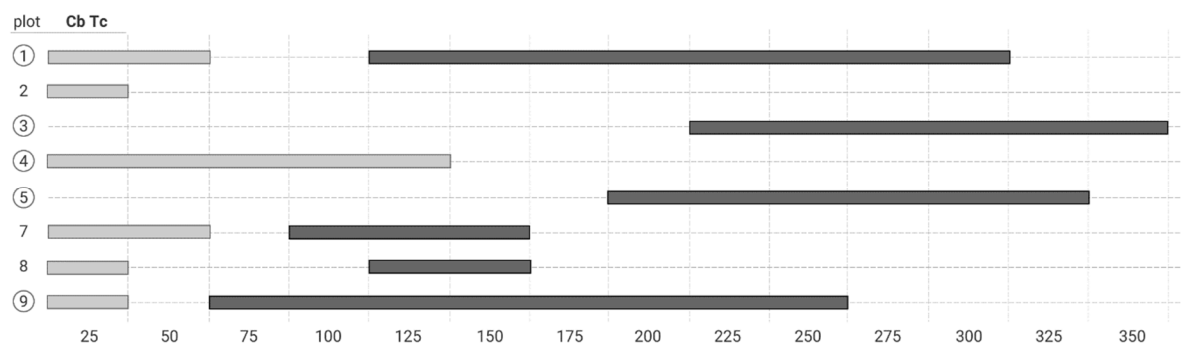


Figure S19. Cb–Tc significant association ranges

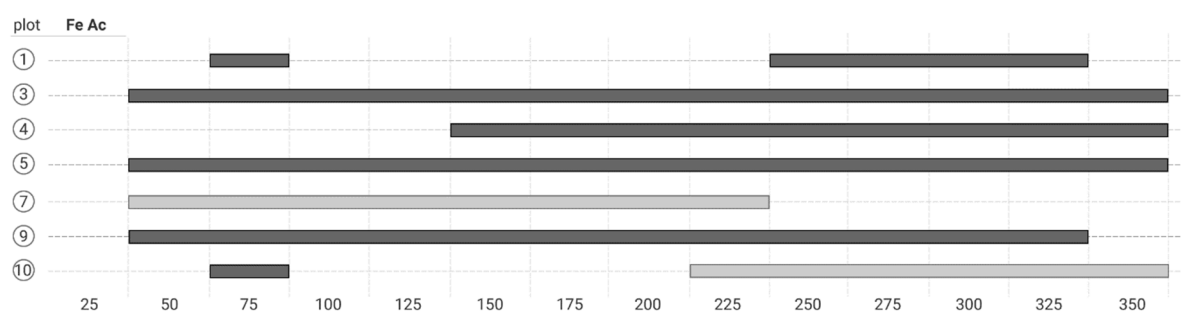


Figure S20. Fe–Ac significant association ranges



Figure S21. Fe–Ap significant association range

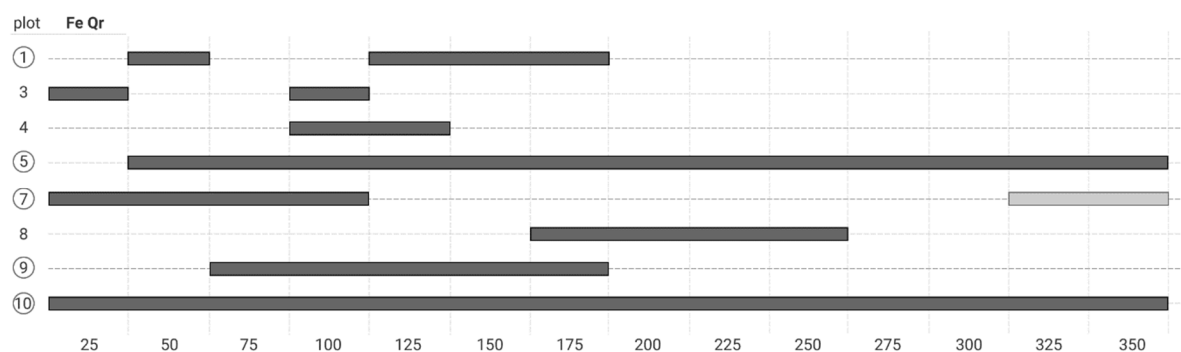


Figure S22. Fe–Qr significant association range

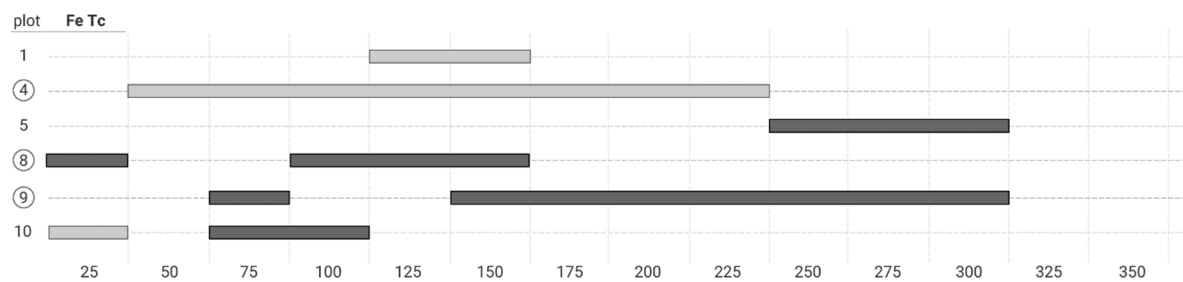


Figure S23. Fe-Tc significant association range

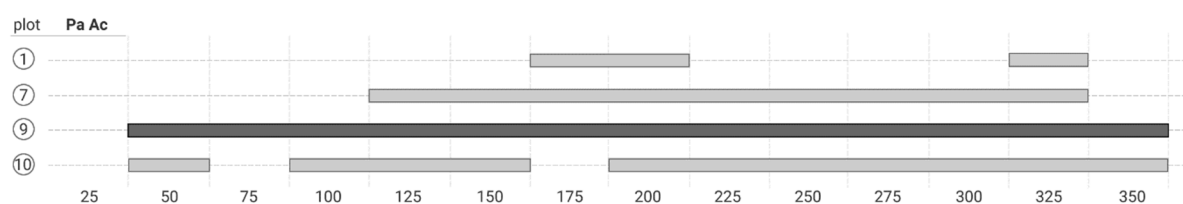


Figure S24. Pa-Ac significant association range

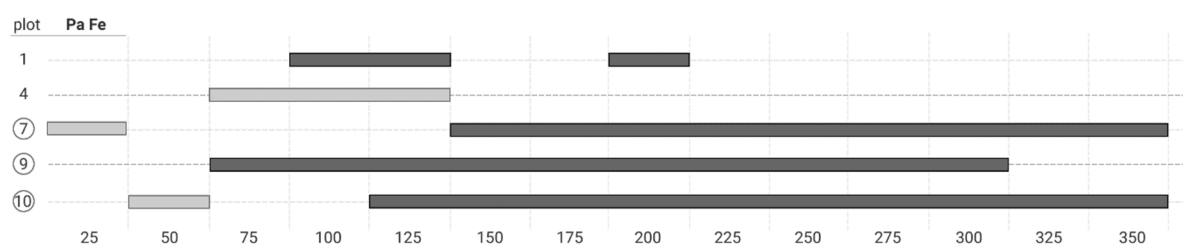


Figure S25. Pa-Fe significant association range

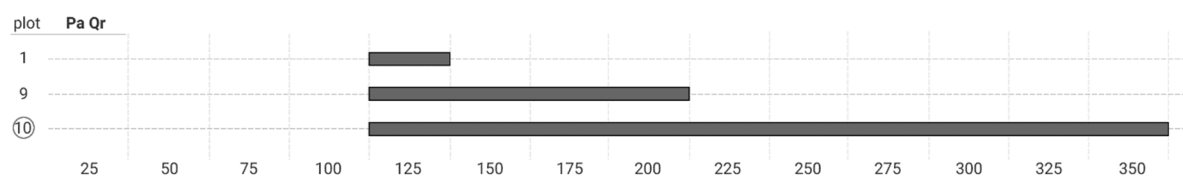


Figure S26. Pa-Qr significant association range

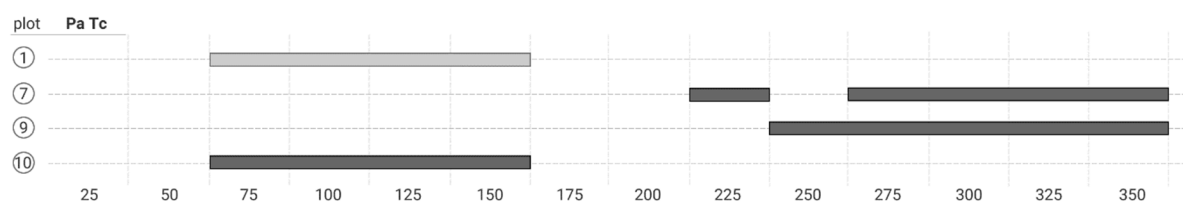


Figure S27. Pa-Tc significant association range

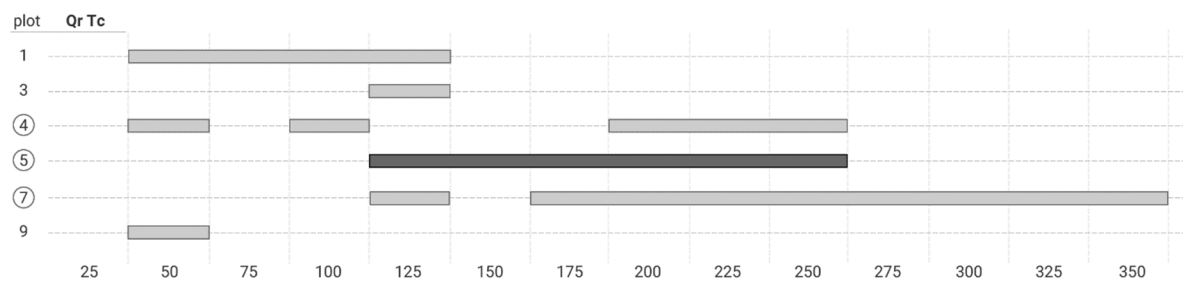


Figure S28. Qr-Tc significant association range

The bivariate $L(t)$ function charts for between-species associations in the analysed plots

Observation: The positive values of $L(t)$ indicate attraction, and the negative ones indicate repulsion among the spatial pattern of the analysed species. The critical confidence envelope at a significance level of 0.05 ($p \leq 0.05$) for the $L(t)$ function was generated using 1000 Monte Carlo simulations. An overall Cramer-von Mises test was applied, assessing the significance level of probability p (higher or lower than 0.05). Distances are given in centimetres.

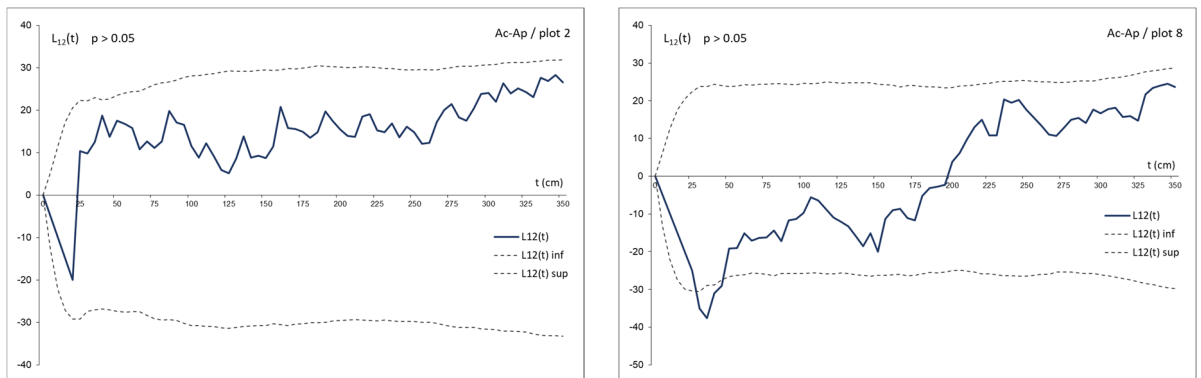
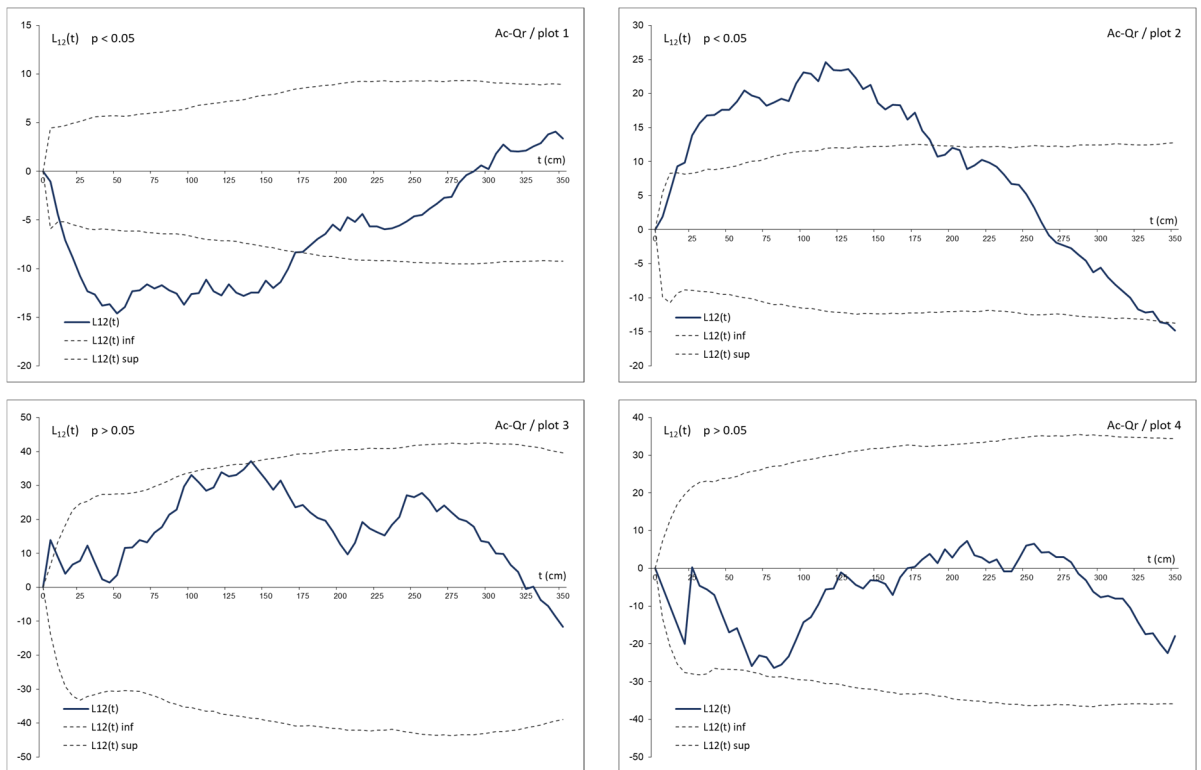


Figure S29. The bivariate $L(t)$ function charts for Ac-Ap pair



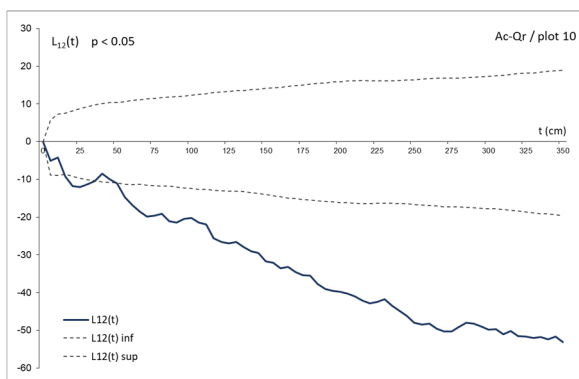
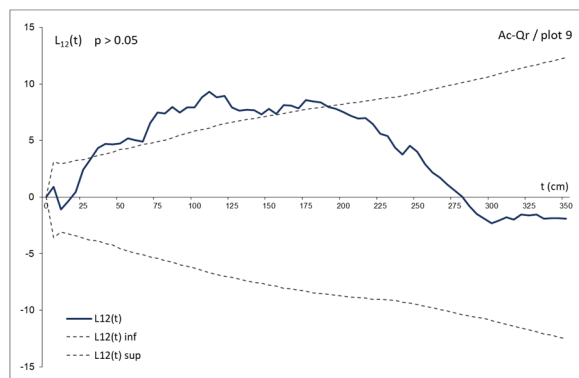
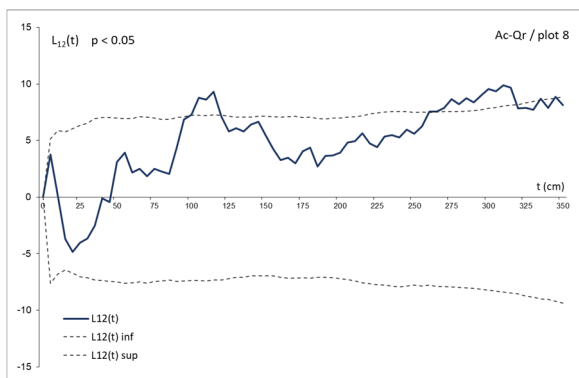
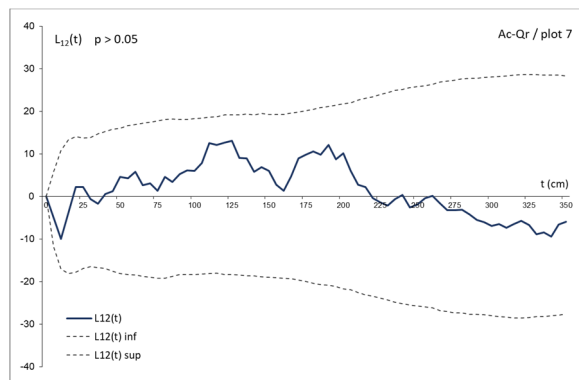
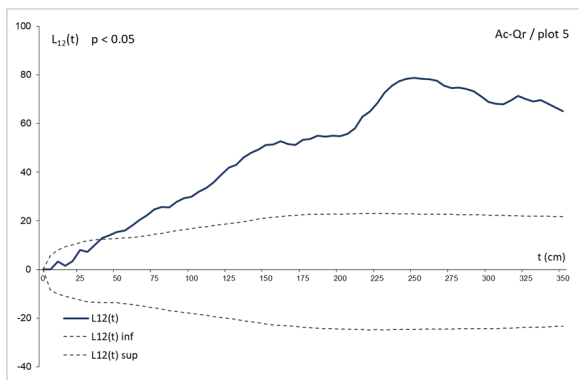
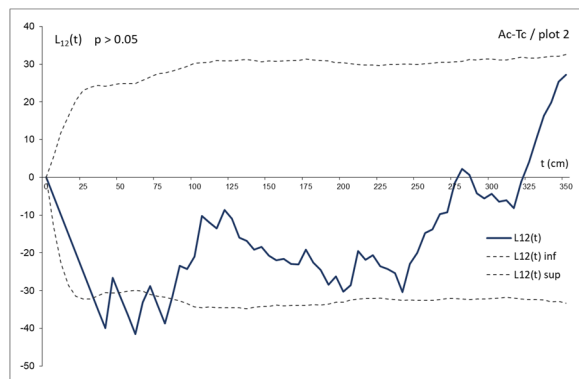
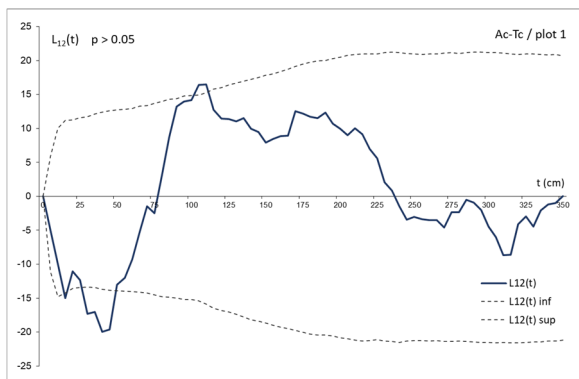


Figure S30. The bivariate $L(t)$ function charts for Ac-Qr pair



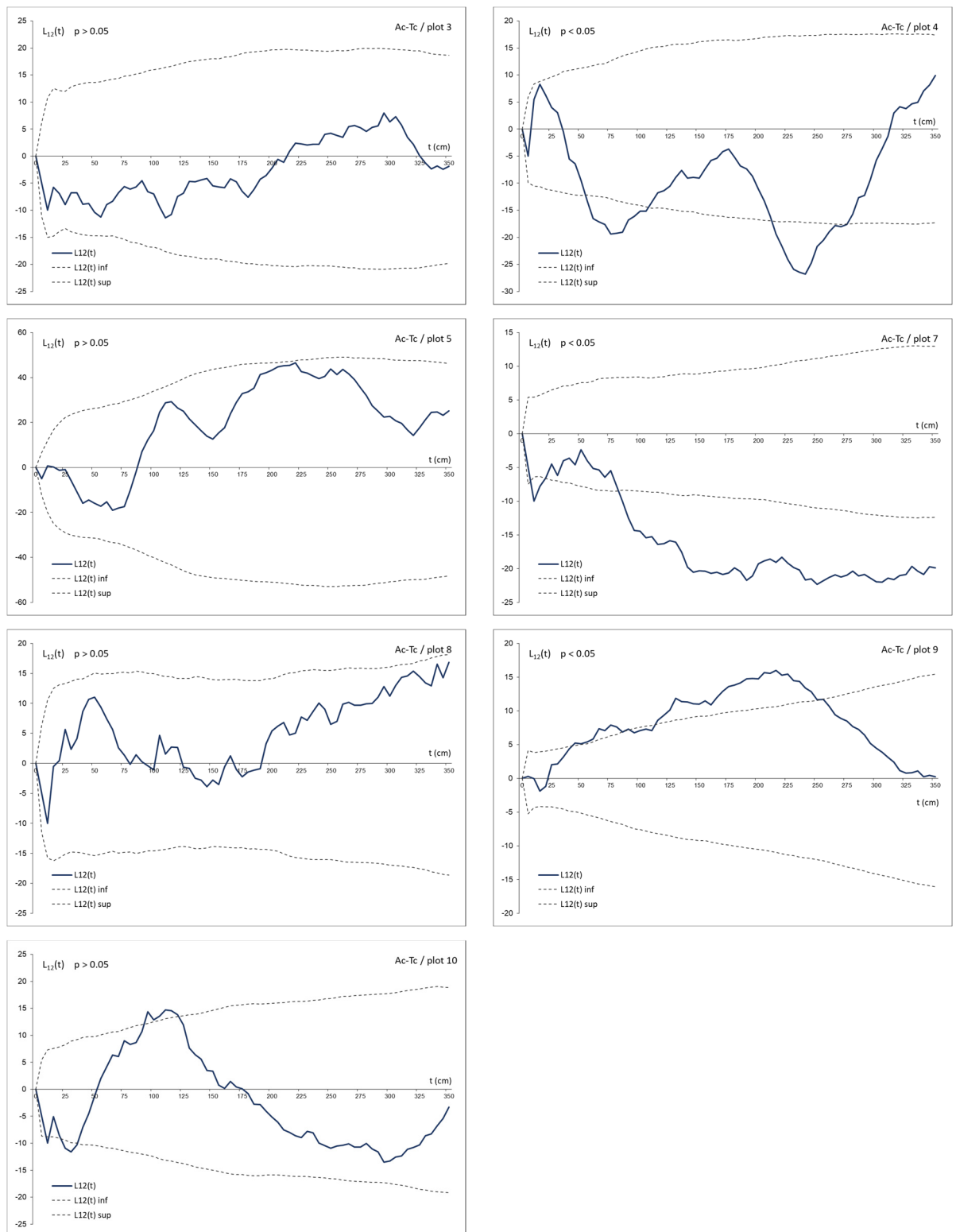


Figure S31. The bivariate $L(t)$ function charts for Ac-Tc pair

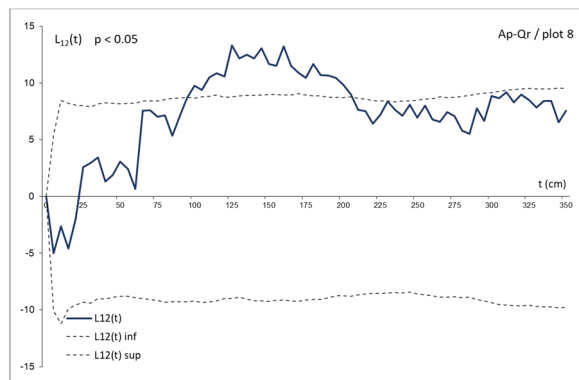
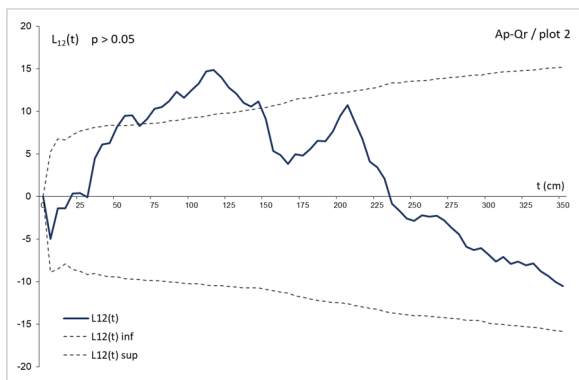


Figure S32. The bivariate $L(t)$ function charts for Ap-Qr pair

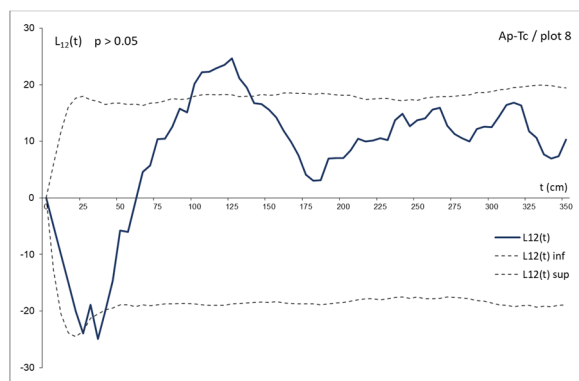
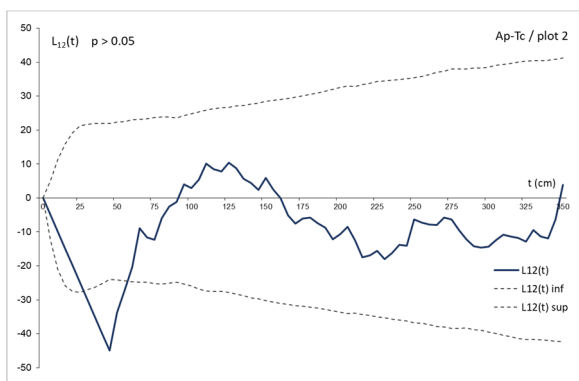
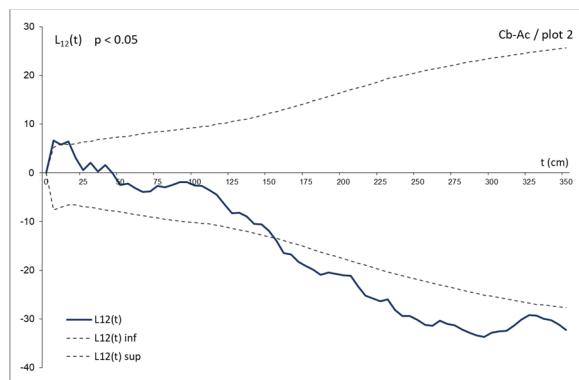
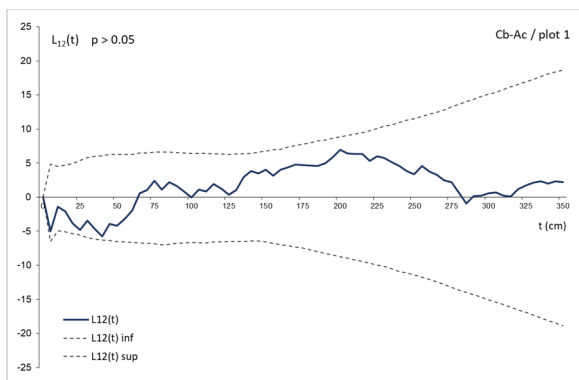


Figure S33. The bivariate $L(t)$ function charts for Ap-Tc pair



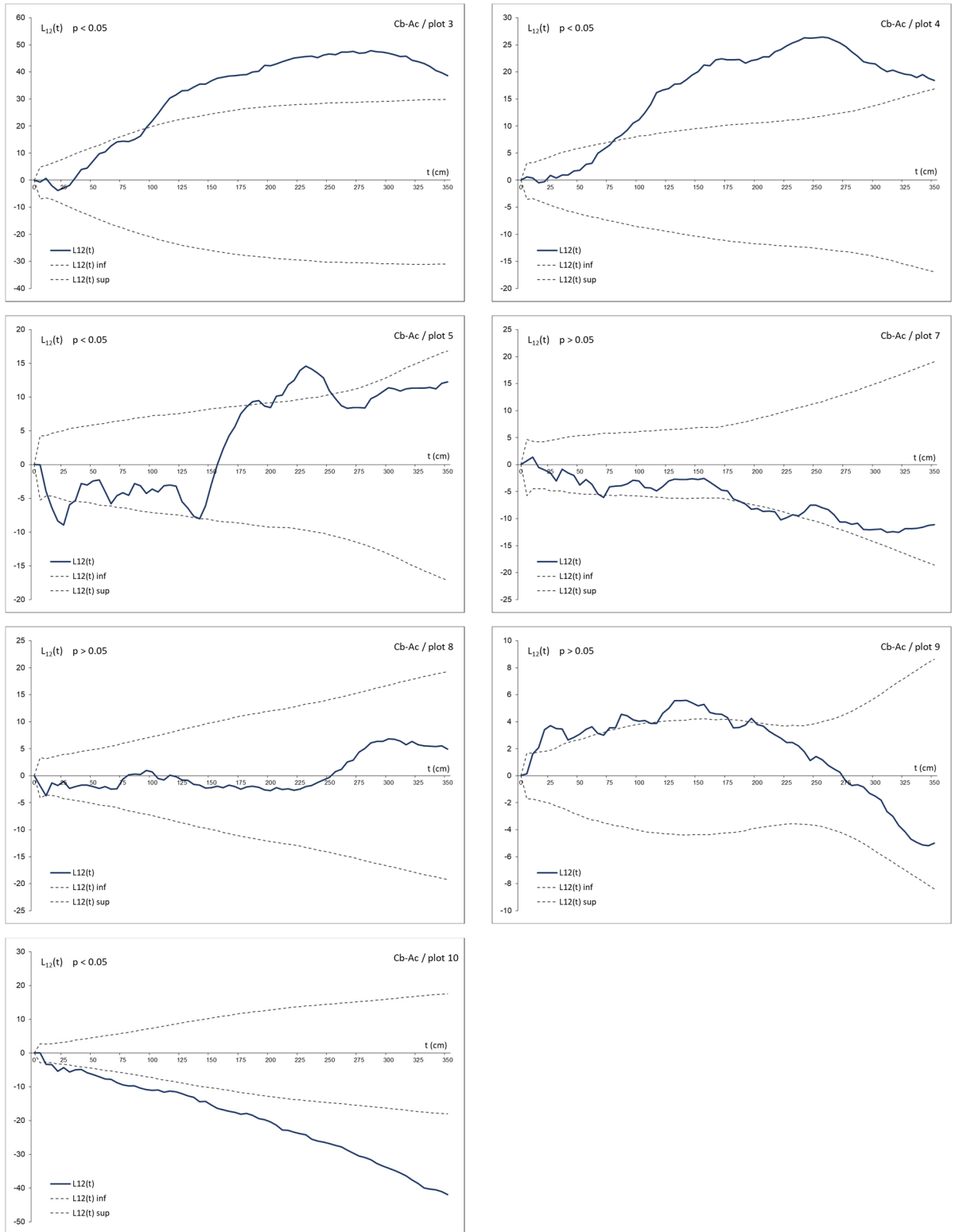


Figure S34. The bivariate $L(t)$ function charts for Cb-Ac pair

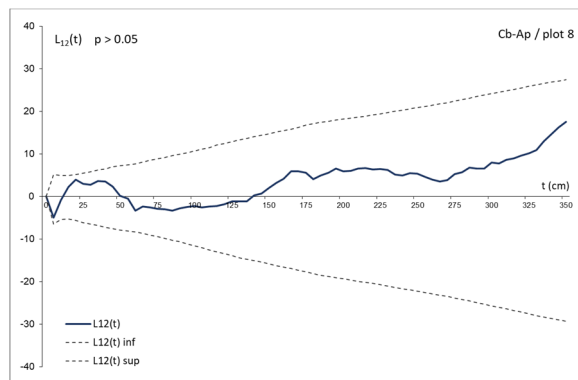
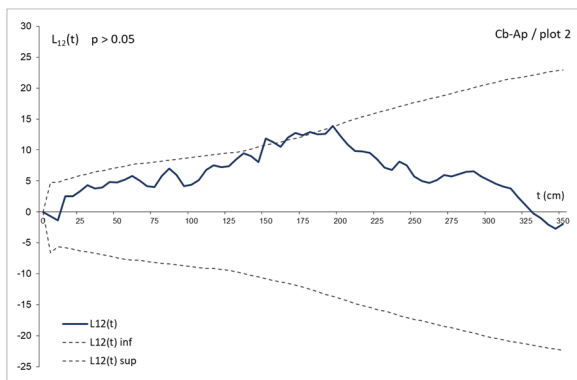
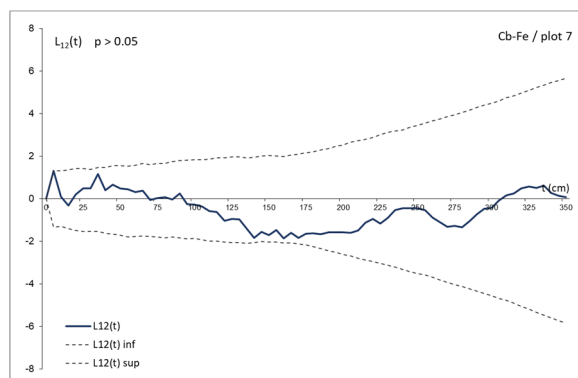
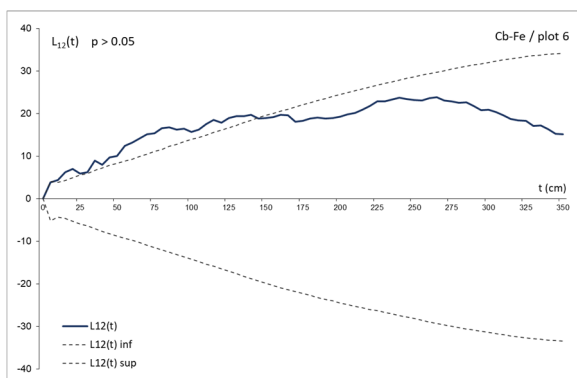
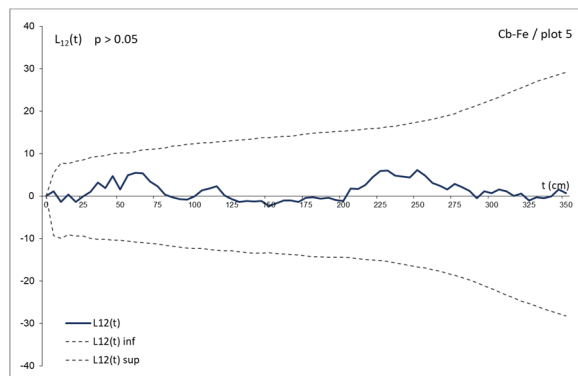
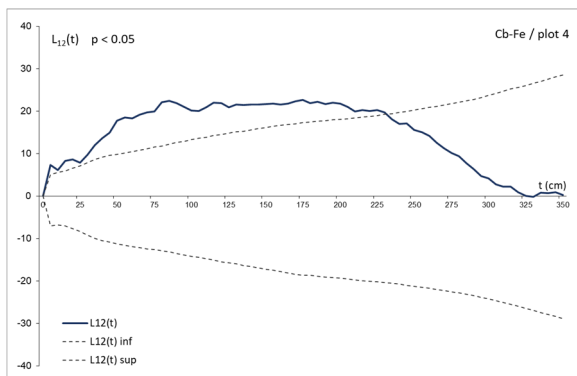
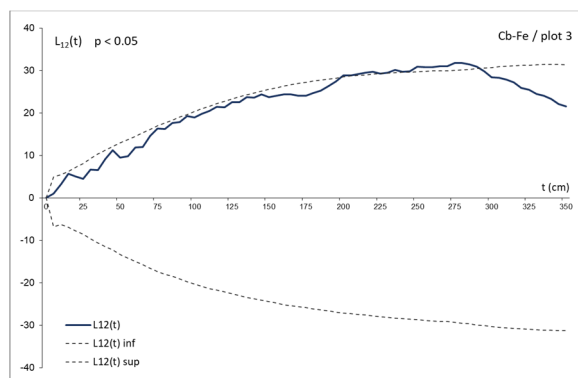
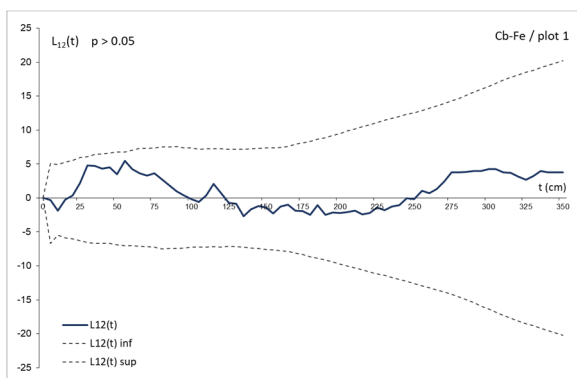


Figure S35. The bivariate $L(t)$ function charts for Cb–Ap pair



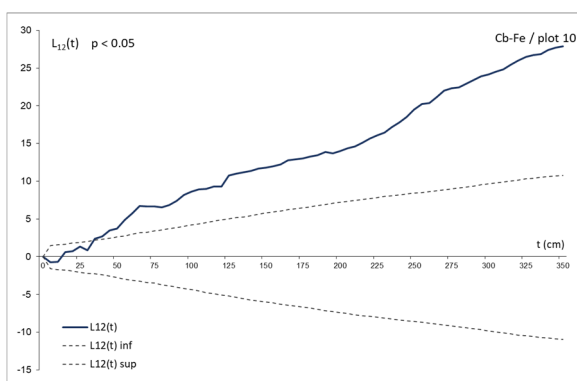
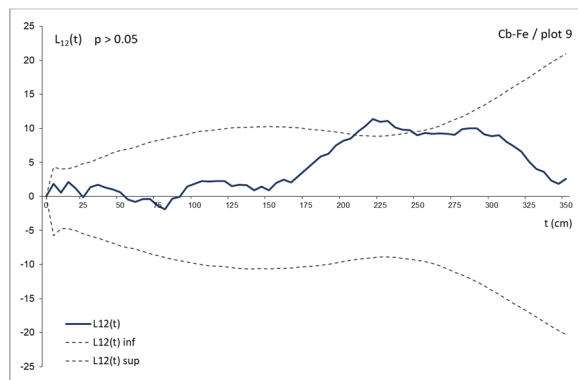
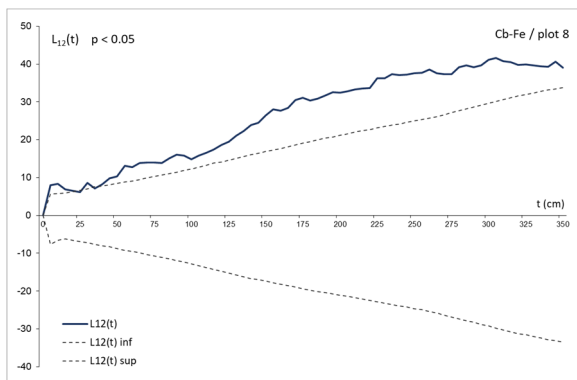
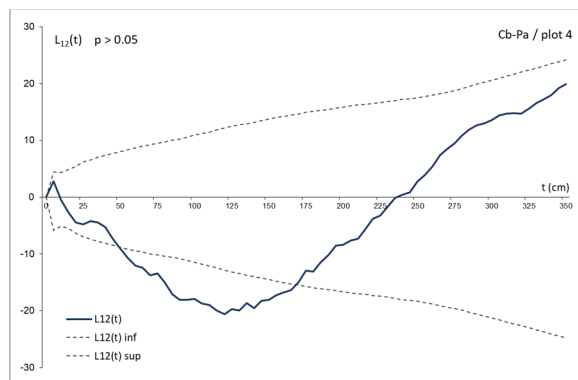
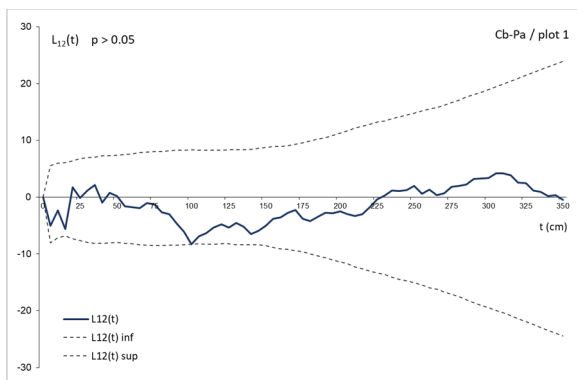


Figure S36. The bivariate $L(t)$ function charts for Cb-Fe pair



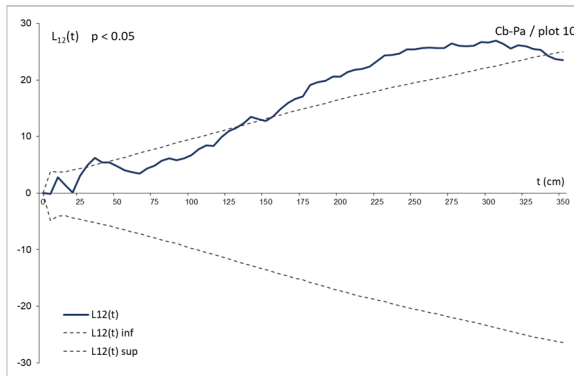
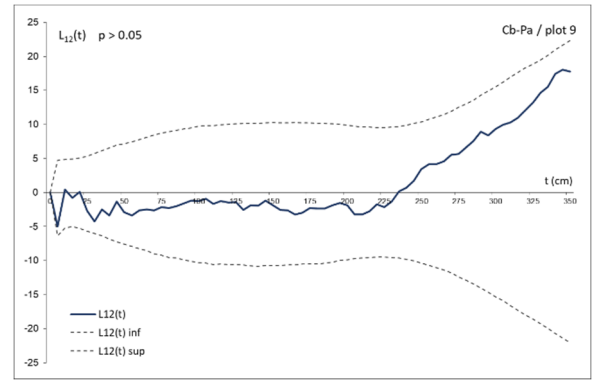
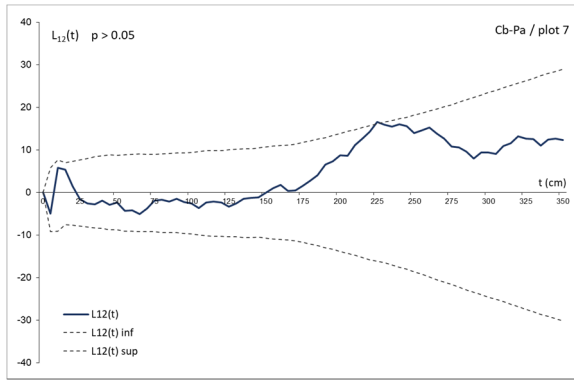
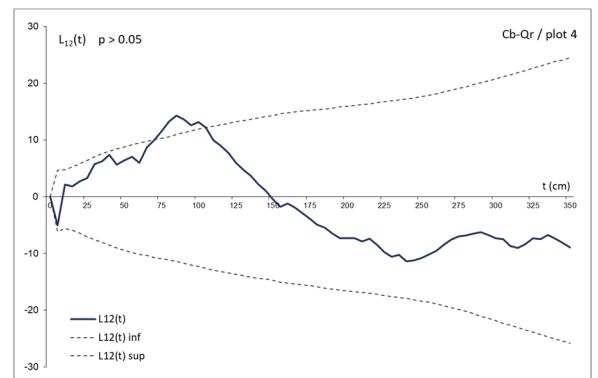
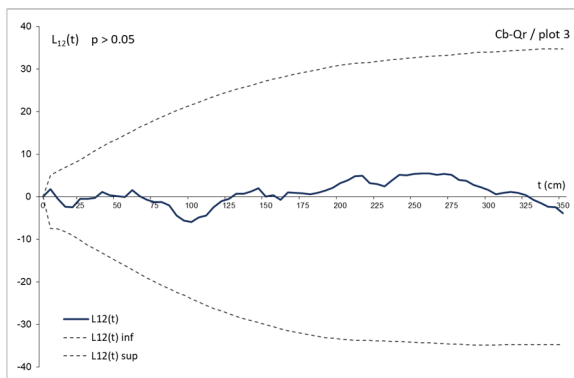
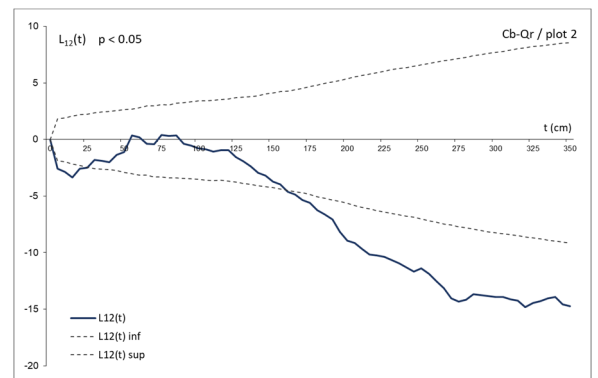
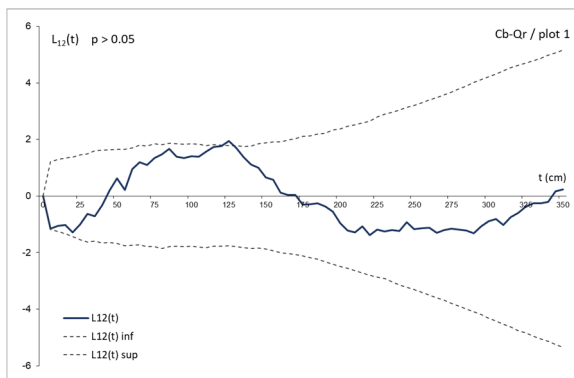


Figure S37. The bivariate $L(t)$ function charts for Cb-Pa pair



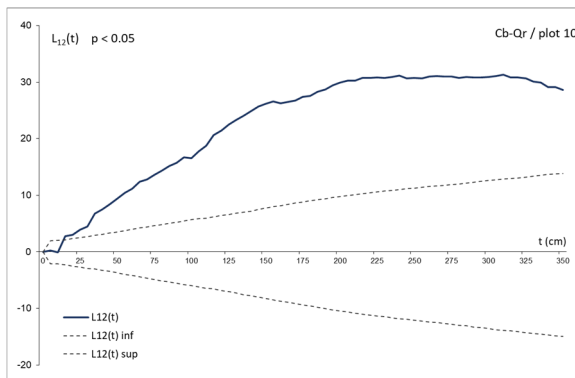
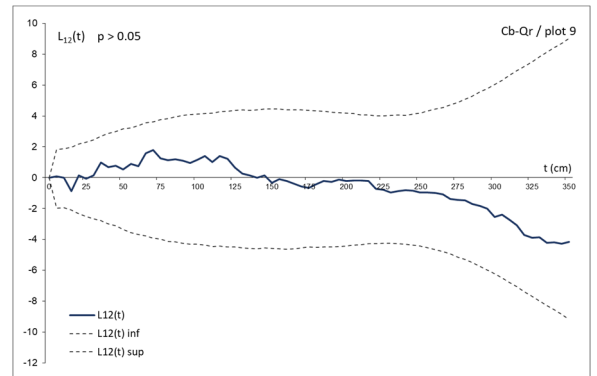
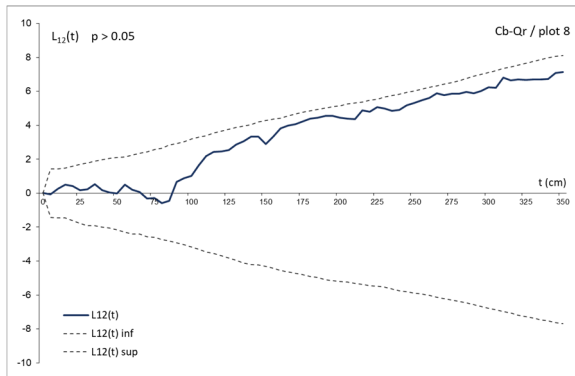
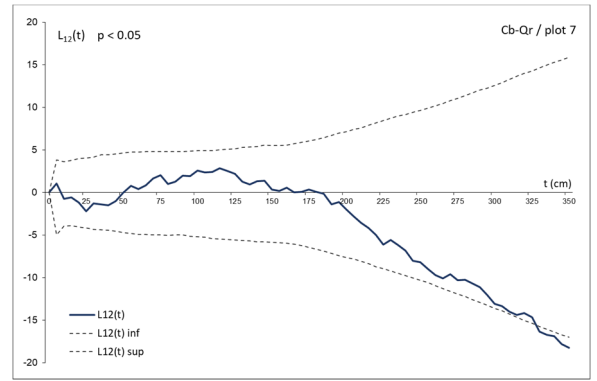
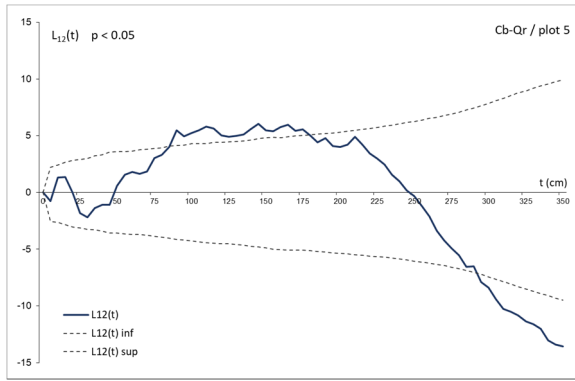
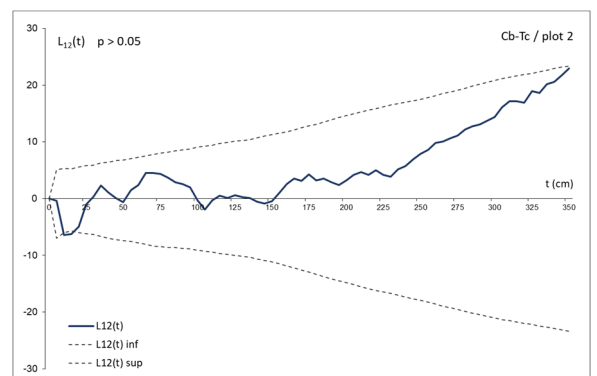
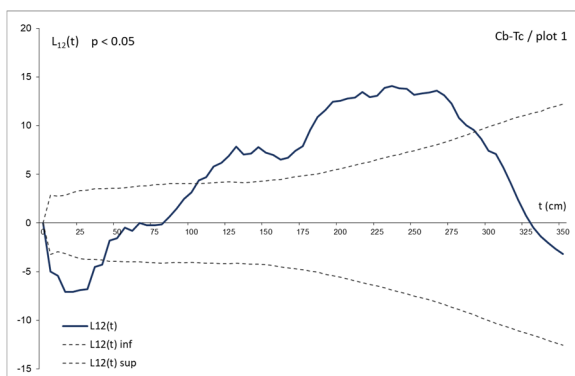


Figure S38. The bivariate $L(t)$ function charts for Cb-Qr pair



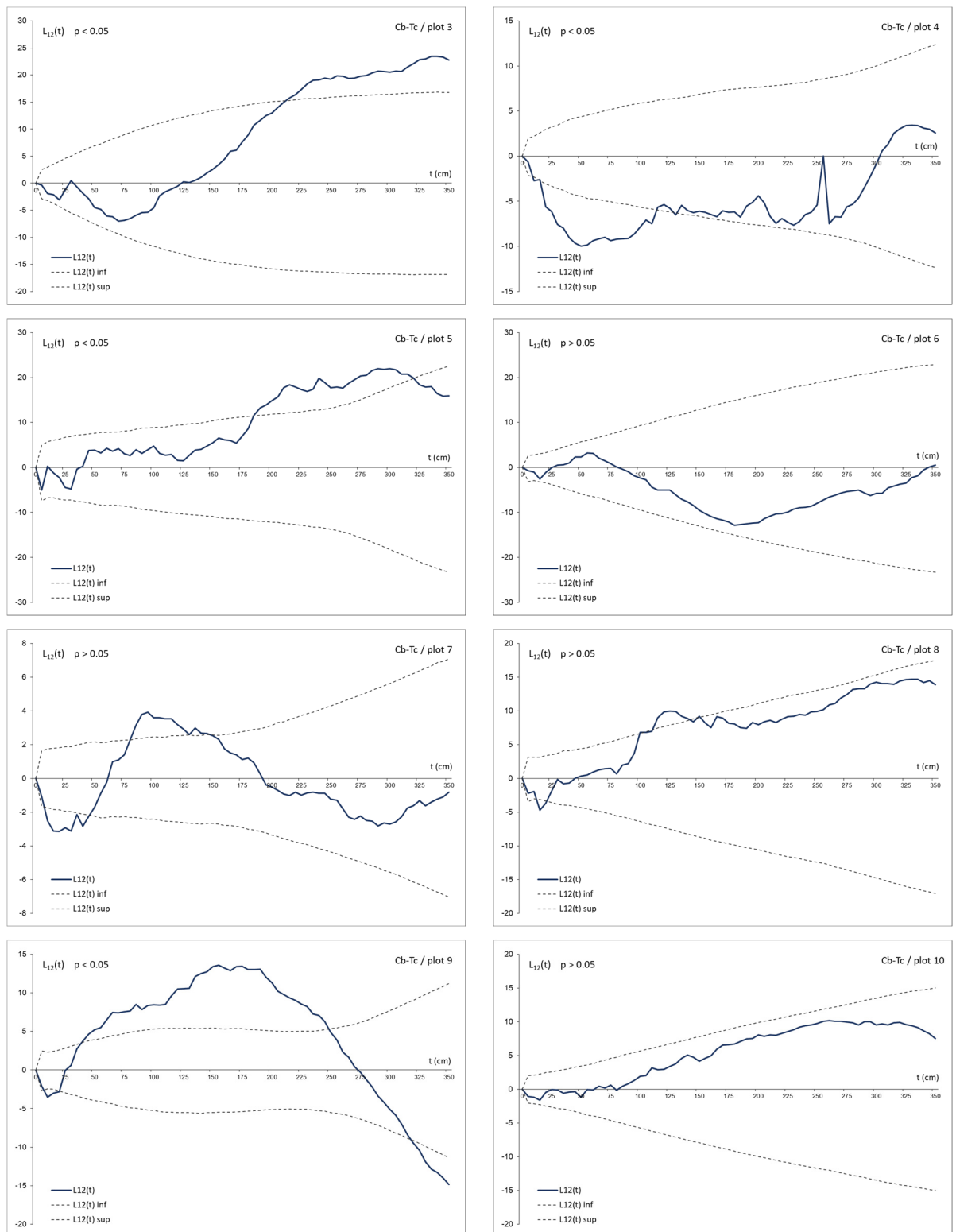


Figure S39. The bivariate $L(t)$ function charts for Cb-Tc pair

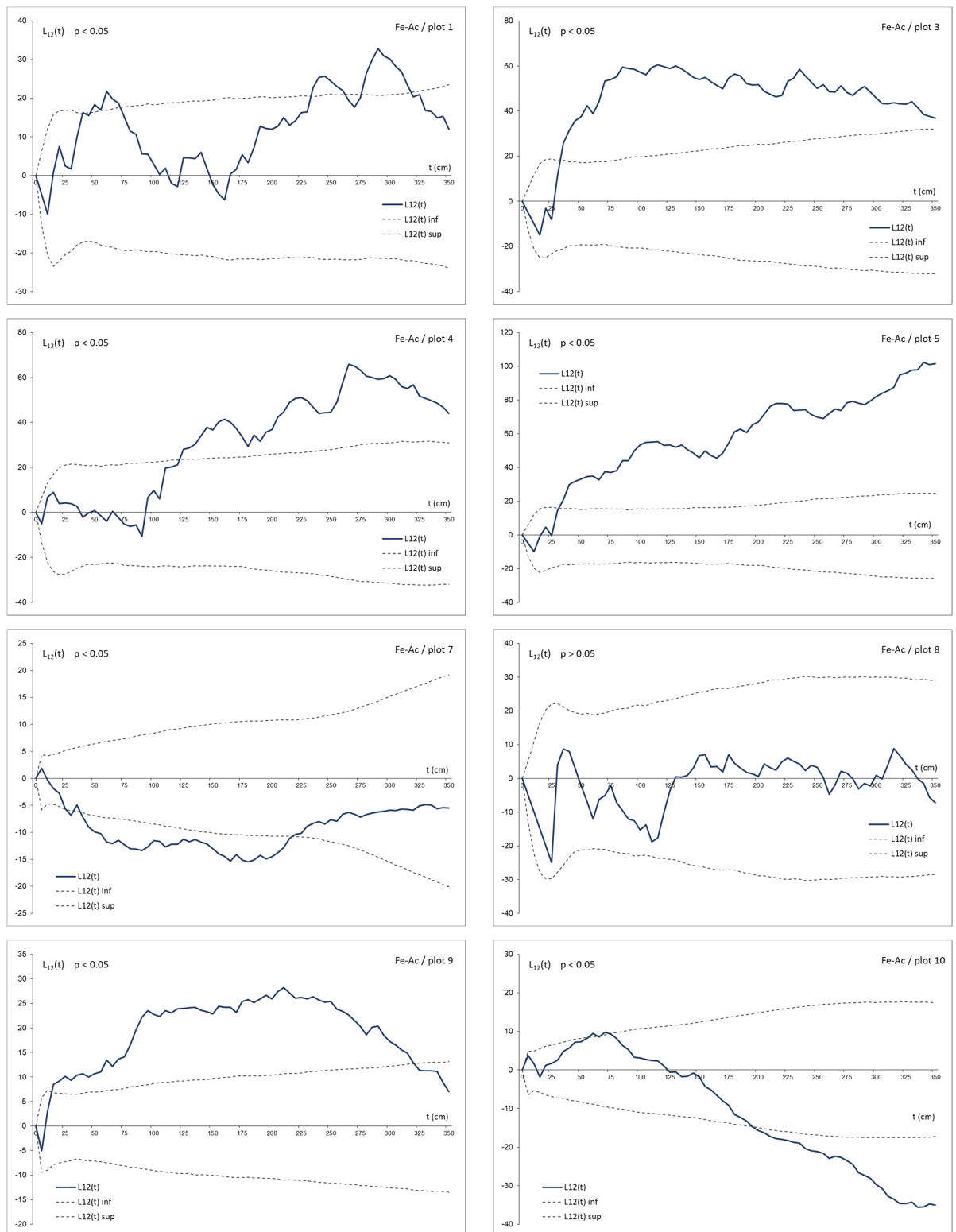


Figure S40. The bivariate $L(t)$ function charts for Fe-Ac pair

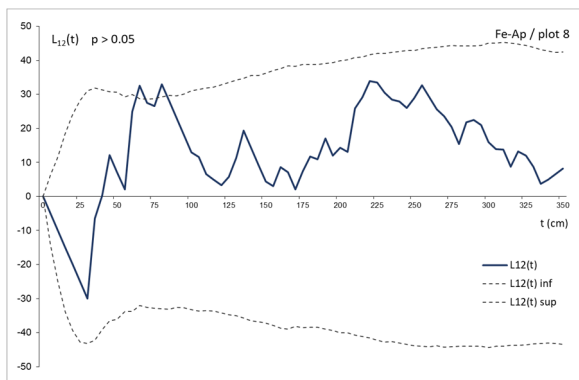
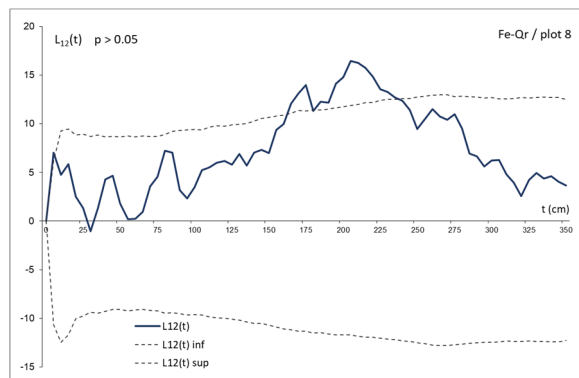
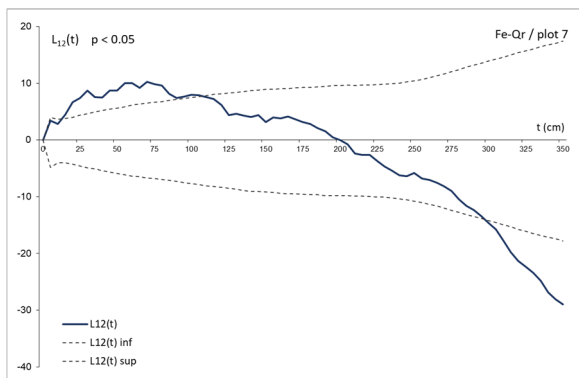
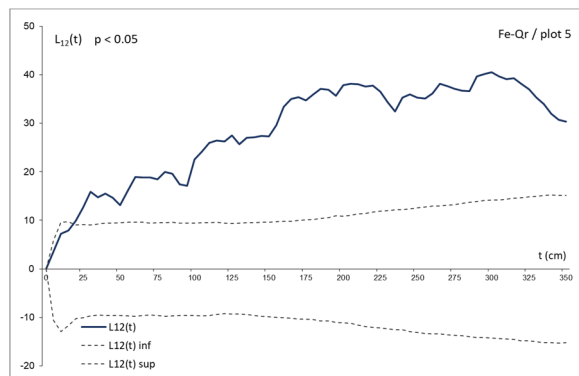
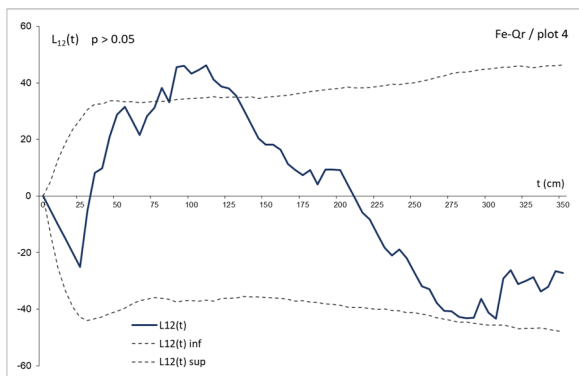
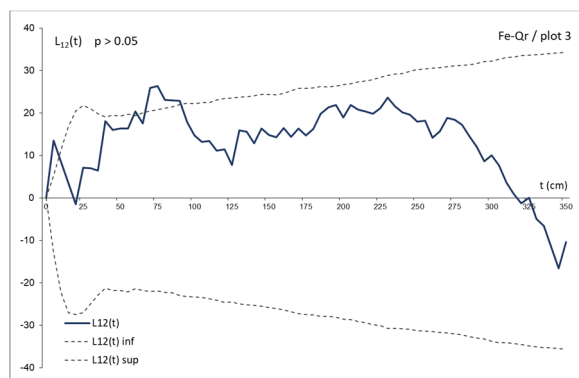
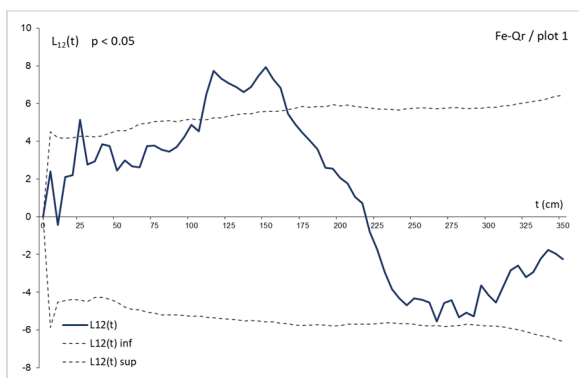


Figure S41. The bivariate $L(t)$ function chart for Fe-Ap pair



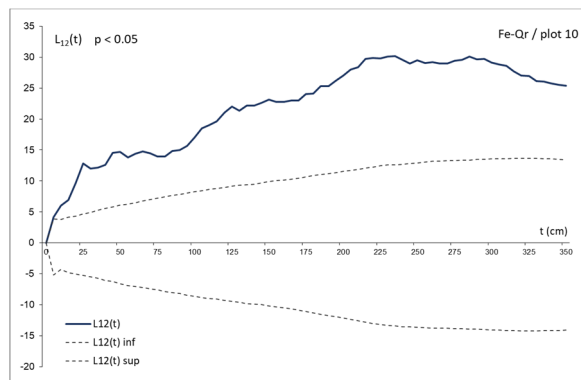
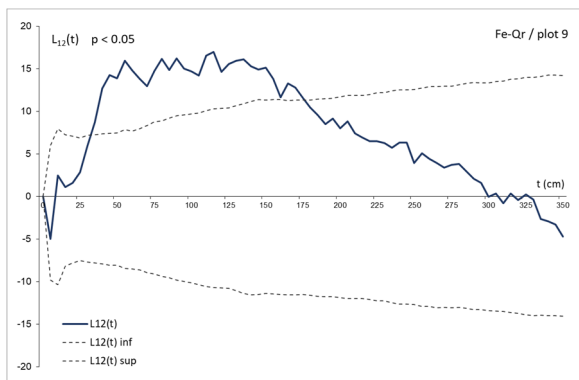
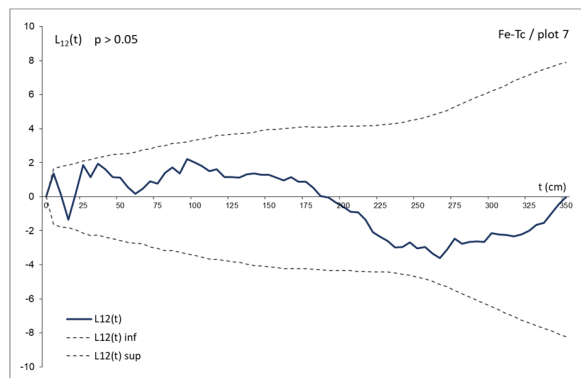
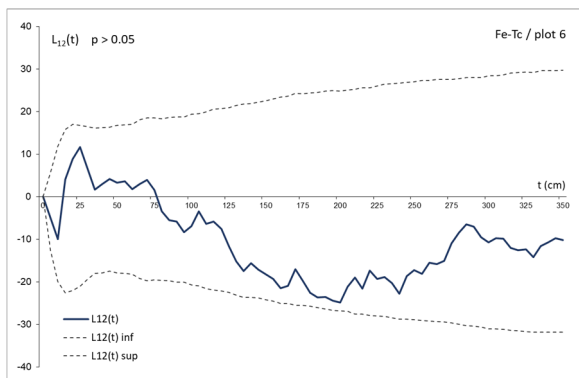
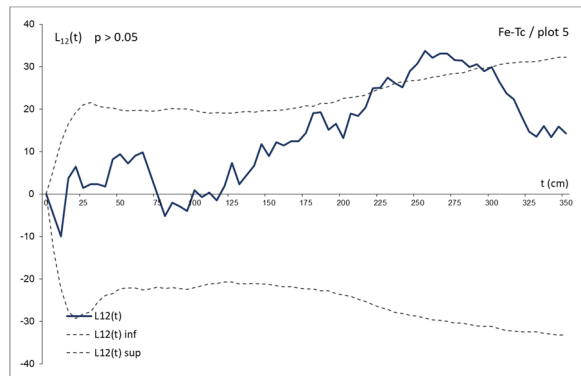
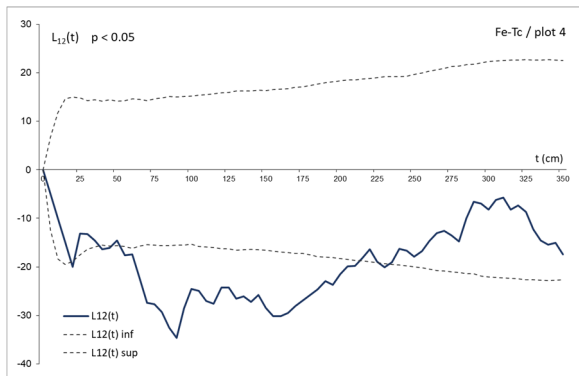
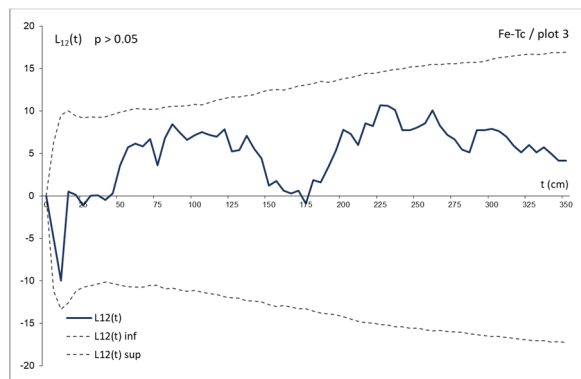
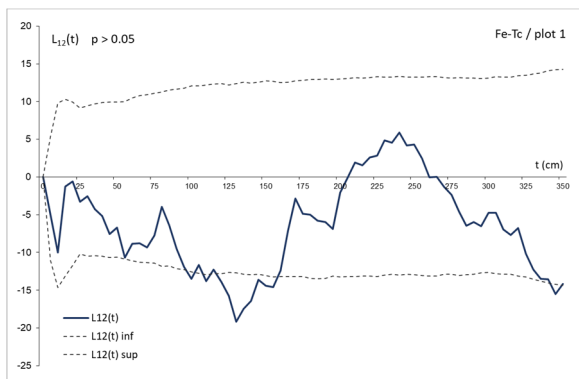


Figure S42. The bivariate $L(t)$ function charts for Fe-Qr pair



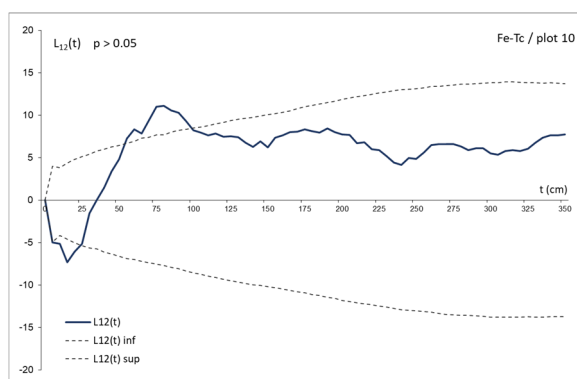
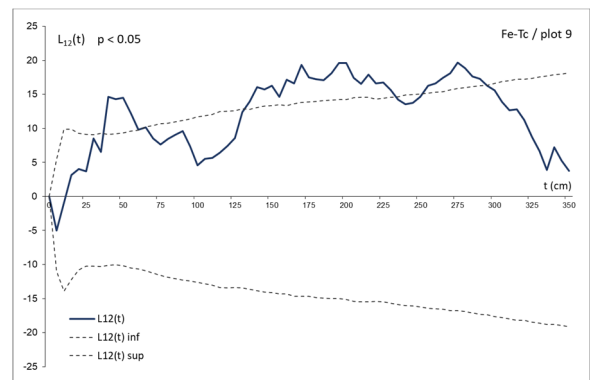
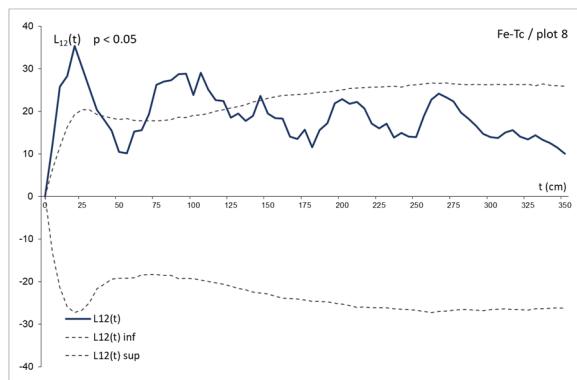


Figure S43. The bivariate $L(t)$ function charts for Fe-Tc pair

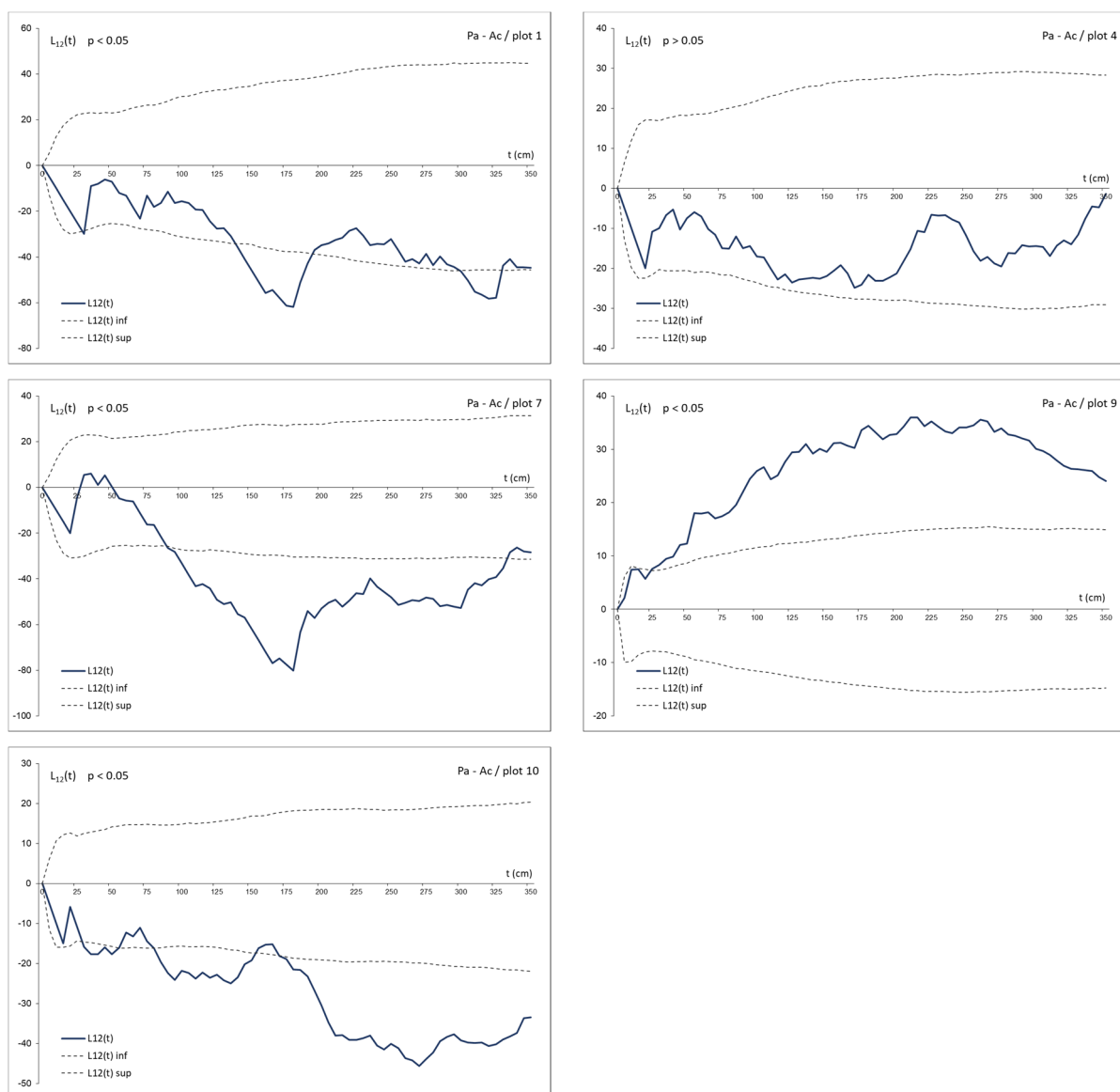


Figure S44. The bivariate $L(t)$ function charts for Pa-Ac pair

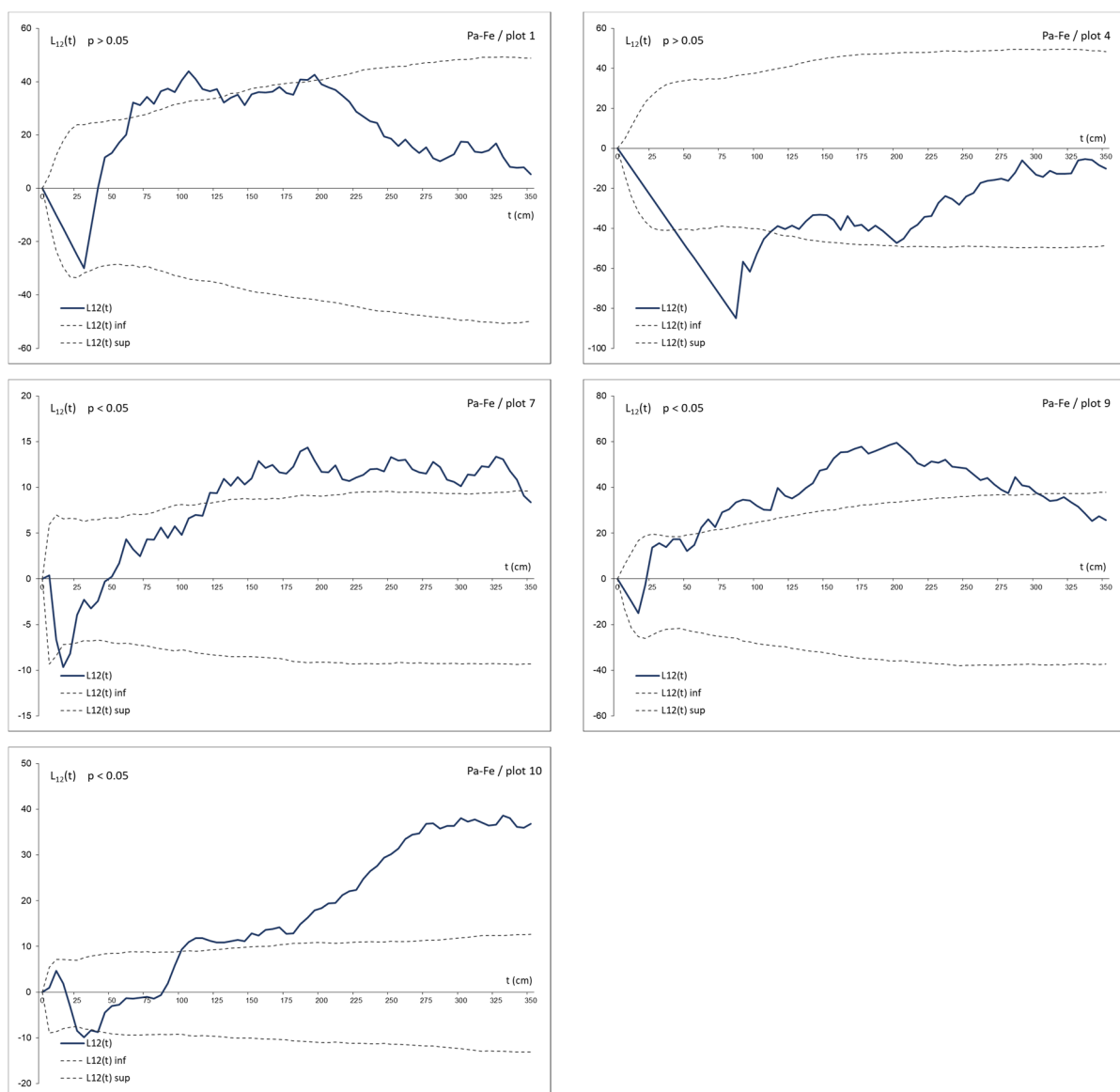


Figure S45. The bivariate $L(t)$ function charts for Pa-Fe pair

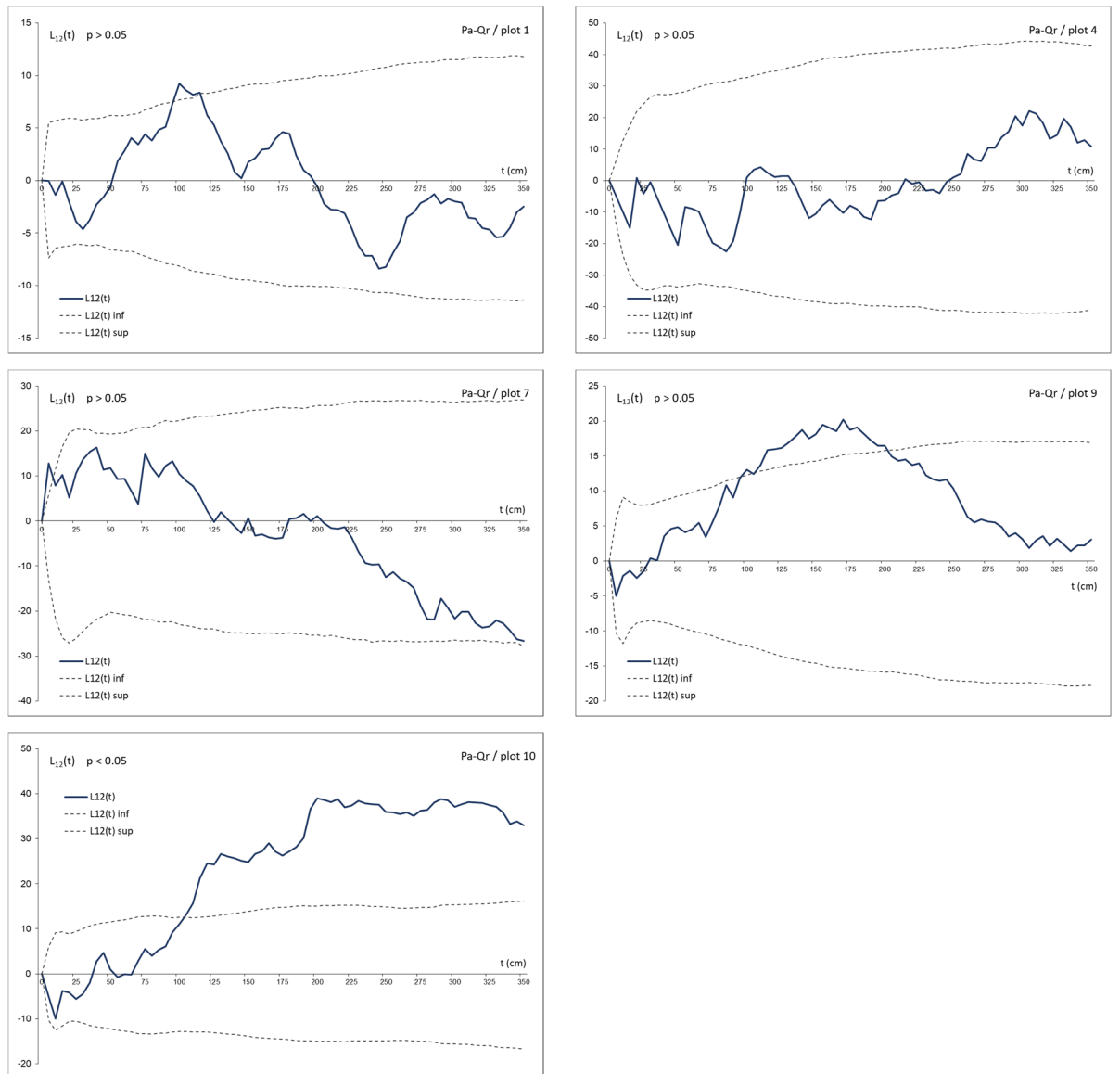


Figure S46. The bivariate $L(t)$ function charts for Pa-Qr pair

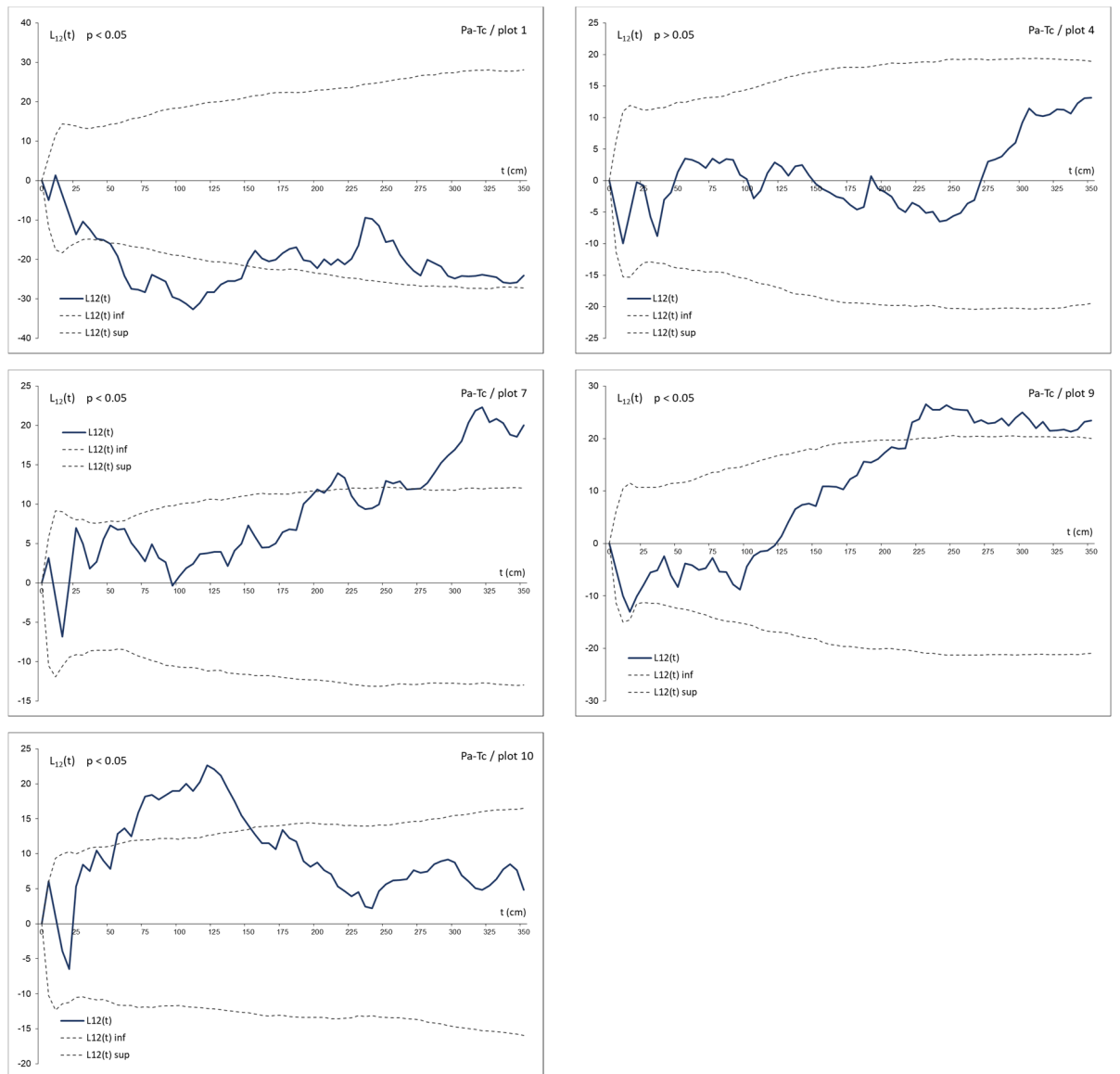
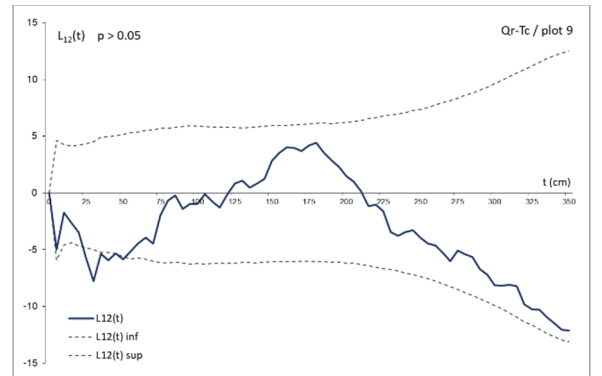
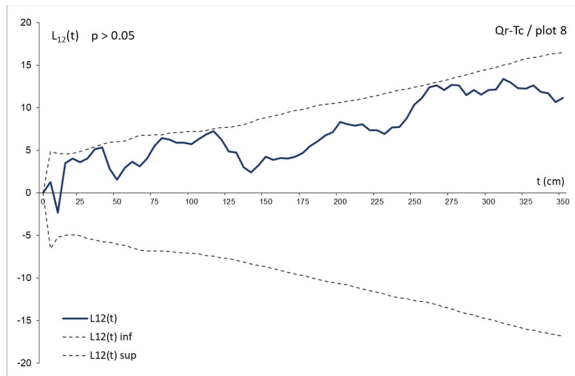
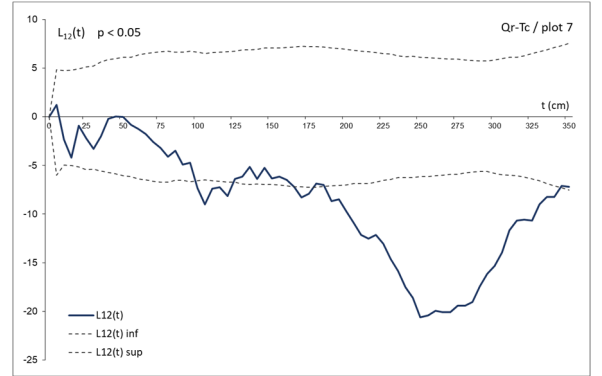
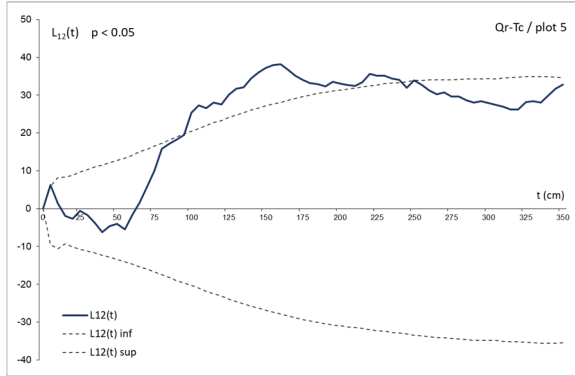
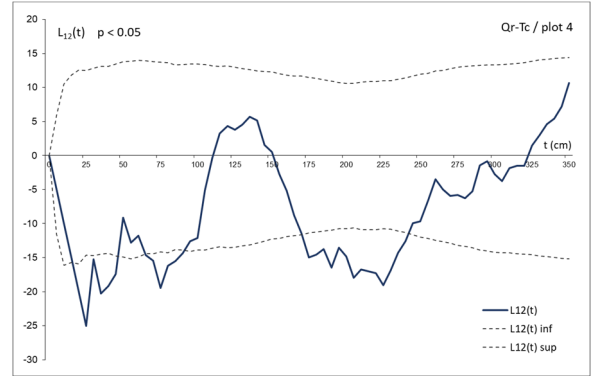
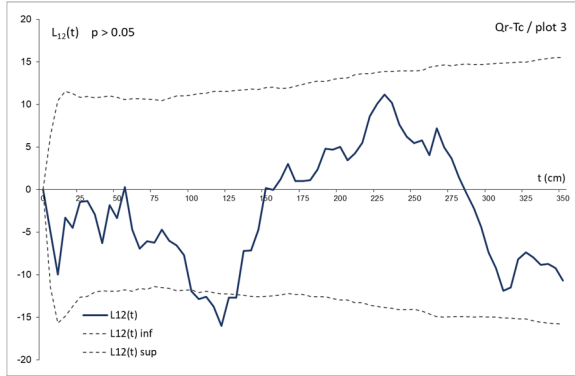
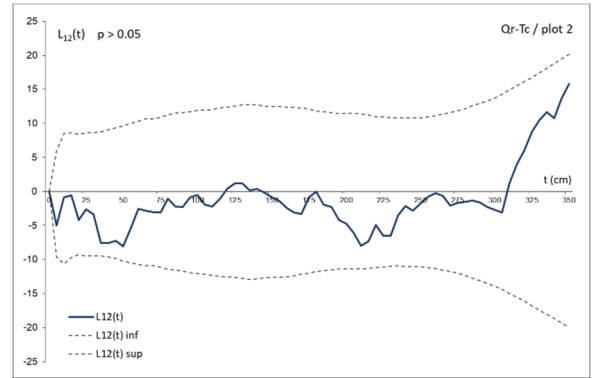
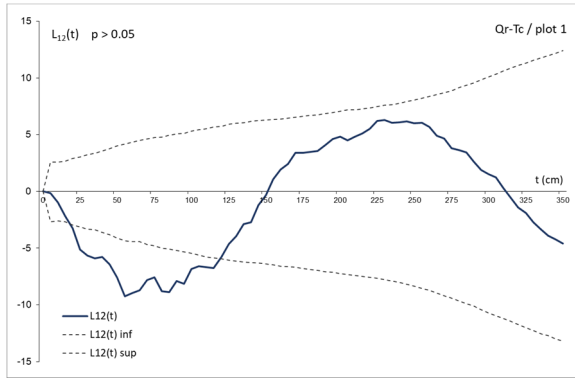


Figure S47. The bivariate $L(t)$ function charts for Pa-Tc pair



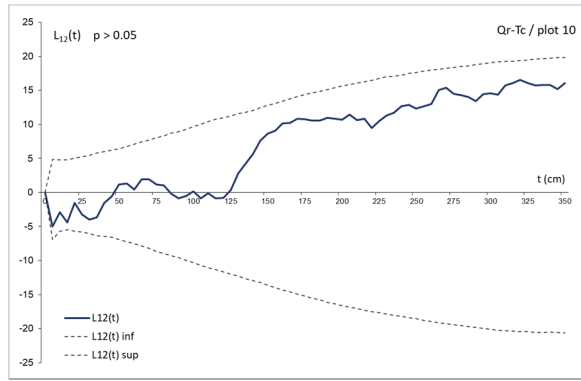


Figure S48. The bivariate $L(t)$ function charts for Qr–Tc pair